higher incidences eating certain foods than control subjects, as follows: ham (2.64 per week/2.42 per week in cases/controls, respectively), squid and shrimp (2.36/2.29), shellfish (2.3/2.03), codfish (2.01/1.76), broccoli (2.95/2.81), green vegetables (4.02/3.69), oranges (3.75/3.30), European cakes (2.02/1.93), black tea (2.15/1.68), coffee (3.47/3.25), vegetables (2.20/1.96), fruit juice (2.03/1.98), beefsteak (1.93/1.86), and grilled chicken (1.81/1.72). On the other hand, there were several foods that were protective against CRC, such as tofu (3.16 per week/3.31 per week in cases/controls, respectively), chicken (2.78/2.92), boiled fish paste (2.33/2.49), and fried foods (2.79/2.87). Without adjustment by age, sex, and location, some of the information might be skewed and could be affected by the food preferences of cases and control subjects.

History of illness and treatment were directly compared between cases and control subjects (Supplementary Table 4). It is worth noting that a history of and a treatment history for DM were observed significantly more frequently in cases than in control subjects ($P = 0.0008$ and $P = 0.040$, respectively). The incidence of gastroduodenal ulcer was higher in control subjects than in cases ($P < 0.0001$). Colon polypectomy was observed more frequently in control subjects than in cases ($P < 0.0001$), which might indicate the importance of the polypectomy to protect from CRC. Epidemiologic data of medications between cases and control subjects were analyzed (Supplementary Table 5). The population of those who received medication and who did not have DM was frequently observed, in 110 of 1511 cases and 113 of 2098 control subjects ($P = 0.0208$). Treatment with nonsteroidal anti-inflammatory drugs was significantly higher in control subjects than in cases. Several previous studies have addressed cyclooxygenase inhibitors and the inhibition of colon polyps.[13,14]

Data in the Supplementary Tables do not consider location, age, or sex, and therefore, we adjusted them and the evaluated data to find actual epidemiologic and environmental risk factors.

Effect of Environmental Factors on CRC Susceptibility after the Correction by Location, Age, and Sex

The results of the epidemiologic study are shown in Table 3A. For body mass index (BMI) at age 20, the OR of CRC among cases with a BMI of > 25 was 1.94 (95% CI 1.25–3.02). The OR for a BMI increment of 1 was 1.05 (95% CI 1.01–1.10) in men. A review of the medical histories revealed that the OR of DM for CRC was 1.50 (95% CI 1.05–2.14) in men. This finding is identical to the previous study by Campbell et al..[7] However, a history of drinking alcohol was not a CRC risk factor in men or women. The OR of cataracts in men was 0.46 (95% CI 0.30–0.72), suggesting that they reflect a protective marker for CRC. With regard to food intake, in particular a higher frequency of consumption of pork and beef (i.e., more than 3 times per week), the OR for CRC was concordantly increased (OR 1.26, 95% CI 1.09–1.47). Vitamin intake was a protective factor for CRC in men (OR 0.69, 95% CI 0.49–0.96).

The OR of two polymorphic sites at rs6983267 on chromosome 8q24 in CRC cases was analyzed with the cohort of 1511 CRC patients and 2098 control subjects (Table 3B). In men, the OR was higher for homozygous variants; however, this did not reach statistical significance (OR 1.36, 95% CI 0.99–1.87). However, in women, there was no significant association between variants of this SNP and the incidence of CRC.

Gene–Environmental Interactions in CRC Morbidity

We examined the interaction between two significant SNPs, such as 8q24.21 and 19q13, and whole environmental factors and found that there was no significant association was observed in 19q13. Therefore, further analysis will be done for the SNP at 8q24.21, rs6983267, in CRC cases.

The genetic–environmental interactions are summarized in Table 4. For rs6983267, the previously described genetic risk allele is the so-called minor or G allele elucidated in CRC cases overall; the genetic nonrisk allele is the major T allele, either homozygous TT or heterozygous GT. In this study, on 8q24 (rs6983267), the theoretical OR that defined the cohort with the so-called nonrisk major alleles TT ($n = 48$) or GT ($n = 44$) specifically in the presence of DM ($n = 11$) had an increased risk for CRC that was 1.66-fold greater than that of the cohort carrying a major allele without DM ($n = 81$). Interestingly, and by contrast, in the presence of DM, there was no association between the occurrence of CRC and the so-called genetic risk or minor allele GG ($n = 18$) (risk 1.03; Table 4).

DISCUSSION

In the current study, we found that the presence of DM and higher BMI at age 20 were risk factors for CRC development, while high tuna and vitamin intake were protective factors against CRC. These four factors were associated with CRC and diabetes in general. Recently, the American Diabetes Association and the American Cancer Society stated that diabetes (primarily type 2) is associated with an increased risk of some cancers, including CRC.[6] They speculated that the association between diabetes and cancer may be due in part to shared risk factors between the two diseases such as aging, obesity, diet, and physical inactivity. Possible mechanisms for a direct link between

TABLE 3 ORs of epidemiologic and genetic factors

Factor	Subfactor	Male		Female		Result
		OR	95% CI	OR	95% CI	
A: Epidemiologic factors						
BMI						
BMI at age 20	>25 vs. < 25	1.94*	1.25–3.02	1.41	0.70–2.86	Risk for men
BMI	Risk at every 1 BMI elevation	1.05*	1.01–1.10	1.02	0.97–1.07	Risk for men
History						
Hypertension	Present vs. absent	1.05	0.81–1.37	1.01	0.72–1.43	
Hyperlipidemia	Present vs. absent	0.92	0.62–1.36	0.77	0.51–1.16	
DM	Present vs. absent	1.5*	1.05–2.14	1.41	0.76–2.59	Risk for men
Cataracts	Present vs. absent	0.46*	0.30–0.72	1.2	0.73–1.98	Risk for men
Chronic hepatitis	Present vs. absent	0.47	0.22–1.02	0.46	0.14–1.51	
Operation history						
Resection of stomach	Yes vs. no	0.46	0.26–0.72	0.5	0.23–1.11	Protective for men
Polypectomy in colon	Yes vs. no	0.79	0.26–1.00	0.66*	0.47–0.92	Protective for women
Cholecystectomy	Yes vs. no	0.57	0.30–1.05	1.31	0.65–2.63	
Cataracta	Yes vs. no	0.73	0.42–1.27	1.3	0.69–2.48	
Smoking history	Smoker vs. nonsmoker	1.18	0.94–1.54	1.21	0.84–1.73	
BI risk	Risk for every 1.0 BI elevation	1.01*	1.00–1.01	1	0.99–1.02	Risk for men
BI value	BI > 30 vs. BI < 30	1.22	0.96–1.53	1.38	0.64–2.99	
Alcohol						
Drinking	Drinker vs. nondrinker	0.95	0.73–1.24	1.15	0.84–1.58	
Consumption	Risk for every 10 g alcohol	0.99	0.97–1.00	0.92	0.83–1.01	
Consumption/d	≥50 g vs. < 50 g	0.91	0.66–1.24	0.31*	0.10–0.97	Protective for women
Food intake						
Beef or pork	≥3 times/week vs. 2 times or less	1.26*	1.09–1.47	0.94	0.79–1.12	Risk for men
Salmon, tuna	≥3 times/week vs. 2 times or less	0.78*	0.67–0.90	0.83*	0.70–0.99	Protective for both
Liver	≥3 times/week vs. 2 times or less	1.11	0.93–1.33	1.1	0.49–1.37	
Drugs, vitamins						
Vitamin intake	Yes vs. no	0.69*	0.49–0.96	0.82	0.57–1.59	Protective for men
Antihypertension medication	Yes vs. no	0.88	0.67–1.15	1.03	0.70–1.49	
Antipyretic analgesic	Yes vs. no	0.5	0.16–1.50	0.9	0.34–2.40	
B: Genetic factors						
8q24	Wild type	1	Reference	1	Reference	1 reference
rs6983267	Heterozygous	1.08	0.88–1.34	0.93	0.71–1.21	1.010.90–1.31
	Homozygous	1.36	0.99–1.87	1.14	0.79–1.64	1.48 1.12–1.95

BI Brinkman index

* Significant at $P < 0.05$

diabetes and cancer include hyperinsulinemia, hyperglycemia, and inflammation. However, they concluded that many research questions remain. These findings are in accord with our current findings, particularly as they relate to the role of diabetes, obesity, and lipid metabolism. However, the OR ratio of those factors was very low (less than 2.0); therefore, it is possible that CRC is provoked not by a single factor (Table 3) but by multiple factors, including interactions among genetic and environmental backgrounds (Table 4).

In spite of the low OR (less than 2.0) for CRC, previous studies have indicated that the 8q24 SNP is a risk allele for various types of malignancies, including CRC.[8,10–12,15–19] A mechanism linking the association between CRC morbidity and 8q24 SNPs has been suspected for some time. Tuupanen et al. demonstrated that the binding affinity of TCF4/LEF for the rs6983267 site, which differed with the polymorphic sequence, defined the transcription level of downstream *MYC* in vitro and in vivo [12]. In other words, the genomic sequence of the risk allele of rs6983267 was

TABLE 4 Interactions between epidemiologic DM and genetic SNP at rs6983267 factors for CRC cases

SNP	DM negative OR (95% CI)	DM positive OR (95% CI)	*P*
8q24 rs6983267			0.043
TT + GT major allele	1 (Ref.)	1.67 (1.19–2.32)	
GG minor allele	1.54 (1.18–2.03)	1.03 (0.48–2.20)	

There is a significant interaction between a history of DM and frequency of rs6983267. Subjects with the major allele and DM had an elevated risk for CRC (1.67 times higher than that of those without DM)

highly homologous with the transcription factor TCF4/LEF; therefore, the transcription of the *MYC* gene was upregulated in CRC cases with the risk allele of rs6983267.

The interaction between the incidence of DM and the difference of allele of rs6983267 at 8q24 was observed to be significant (Table 4). However, the risk for CRC was upregulated in CRC cases with DM plus the nonrisk allele of rs6983267. The risk allele of rs6983267 did not elevate the risk for CRC in DM cases. We speculate as follows that for risky allele cases, the oncogenic risk for CRC was enough and the risk reached a ceiling; therefore, DM did not elevate the risk for CRC anymore. Nonrisk allele cases and DM could enhance the risk for CRC by 1.67 times only with the presence of the nonrisk allele for CRC.

In conclusion, we report that the rs6983267 SNP at 8q24 is a cancer-associated polymorphism. We also verified environmental risk factors for CRC, such as DM, high meat consumption, and higher BMI at age 20. We initially observed a risk for CRC through interactions between the genetic background and environmental factors (e.g., DM). The extremely low OR for CRC suggests that CRC might be provoked by the presence of multiple and diverse risk factors.

ACKNOWLEDGMENT This work was supported in part by the following grants and foundations: CREST, Japan Science and Technology Agency (JST); Japan Society for the Promotion of Science (JSPS) Grant-in-Aid for Scientific Research, grant numbers 20390360, 20591547, 20790960, 21591644, 21791295, 21791297, 215921014 and 21679006; and the Funding Program for Next Generation World-Leading Researchers (LS094); and NEDO (New Energy and Industrial Technology Development Organization) Technological Development for Chromosome Analysis.

REFERENCES

1. Zanke BW, Greenwood CM, Rangrej J, et al. Genome-wide association scan identifies a colorectal cancer susceptibility locus on chromosome 8q24. *Nat Genet.* 2007;39:989–94.
2. Tomlinson IP, Webb E, Carvajal-Carmona L, et al. A genome-wide association study identifies colorectal cancer susceptibility loci on chromosomes 10p14 and 8q23.3. *Nat Genet.* 2008;40:623–30.
3. Tenesa A, Farrington SM, Prendergast JG, et al. Genome-wide association scan identifies a colorectal cancer susceptibility locus on 11q23 and replicates risk loci at 8q24 and 18q21. *Nat Genet.* 2008;40:631–7.
4. Wijnen JT, Brohet RM, van Eijk R, et al. Chromosome 8q23.3 and 11q23.1 variants modify colorectal cancer risk in Lynch syndrome. *Gastroenterology.* 2009;136:131–7.
5. Houlston RS, Webb E, Broderick P, et al. Meta-analysis of genome-wide association data identifies four new susceptibility loci for colorectal cancer. *Nat Genet.* 2008;40:1426–35.
6. Giovannucci E, Harlan DM, Archer MC, et al. Diabetes and cancer: a consensus report. *CA Cancer J Clin.* 2010;60:207–21.
7. Campbell PT, Deka A, Jacobs EJ, et al. Prospective study reveals associations between colorectal cancer and type 2 diabetes mellitus or insulin use in men. *Gastroenterology.* 139:1138–46.
8. Tuupanen S, Niittymaki I, Nousiainen K, et al. Allelic imbalance at rs6983267 suggests selection of the risk allele in somatic colorectal tumor evolution. *Cancer Res.* 2008;68:14–7.
9. Thompson CL, Plummer SJ, Acheson LS, Tucker TC, Casey G, Li L. Association of common genetic variants in SMAD7 and risk of colon cancer. *Carcinogenesis.* 2009;30:982–6.
10. Berndt SI, Potter JD, Hazra A, et al. Pooled analysis of genetic variation at chromosome 8q24 and colorectal neoplasia risk. *Hum Mol Genet.* 2008;17:2665–72.
11. Tomlinson I, Webb E, Carvajal-Carmona L, et al. A genome-wide association scan of tag SNPs identifies a susceptibility variant for colorectal cancer at 8q24.21. *Nat Genet.* 2007;39:984–8.
12. Tuupanen S, Turunen M, Lehtonen R, et al. The common colorectal cancer predisposition SNP rs6983267 at chromosome 8q24 confers potential to enhanced Wnt signaling. *Nat Genet.* 2009;41:885–90.
13. Koehne CH, Dubois RN. COX-2 inhibition and colorectal cancer. *Semin Oncol.* 2004;31:12–21.
14. North GL. Celecoxib as adjunctive therapy for treatment of colorectal cancer. *Ann Pharmacother.* 2001;35:1638–43.
15. Li L, Plummer SJ, Thompson CL, et al. A common 8q24 variant and the risk of colon cancer: a population-based case-control study. *Cancer Epidemiol Biomarkers Prev.* 2008;17:339–42.
16. Curtin K, Lin WY, George R, et al. Meta association of colorectal cancer confirms risk alleles at 8q24 and 18q21. *Cancer Epidemiol Biomarkers Prev.* 2009;18:616–21.
17. Haiman CA, Le Marchand L, Yamamato J, et al. A common genetic risk factor for colorectal and prostate cancer. *Nat Genet.* 2007;39:954–6.
18. Pomerantz MM, Ahmadiyeh N, Jia L, et al. The 8q24 cancer risk variant rs6983267 shows long-range interaction with MYC in colorectal cancer. *Nat Genet.* 2009;41:882–4.
19. Yeager M, Xiao N, Hayes RB, et al. Comprehensive resequence analysis of a 136 kb region of human chromosome 8q24 associated with prostate and colon cancers. *Hum Genet.* 2008;124:161–70.

Transcriptomic study of dormant gastrointestinal cancer stem cells

SHIMPEI NISHIKAWA[1,2], DYAH LAKSMI DEWI[1,2], HIDESHI ISHII[1], MASAMITSU KONNO[1], NAOTSUGU HARAGUCHI[1], YOSHIHIRO KANO[1,2], TAKAHITO FUKUSUMI[1,2], KATSUYA OHTA[1,2], YUKO NOGUCHI[1,2], MIYUKI OZAKI[1,2], DAISUKE SAKAI[1], TAROH SATOH[1], YUICHIRO DOKI[2] and MASAKI MORI[2]

Departments of [1]Frontier Science for Cancer and Chemotherapy and [2]Gastroenterological Surgery, Osaka University, Graduate School of Medicine, Suita, Osaka 565-0871, Japan

Received March 5, 2012; Accepted May 16, 2012

DOI: 10.3892/ijo.2012.1531

Abstract. We previously discovered the coexistence of dormant and proliferating cancer stem cells (CSCs) in gastrointestinal cancer, which leads to chemoradiation resistance. $CD13^-/CD90^+$ proliferating liver CSCs are sensitive to chemotherapy, and $CD13^+/CD90^-$ dormant CSCs have a limited proliferation ability, survive in hypoxic areas with reduced oxidative stress, and relapse and metastasize to other organs. In such $CD13^+$ dormant cells, non-homologous end-joining, an error-prone repair mechanism, is dominant after DNA damage, whereas high-fidelity homologous recombination is apparent in $CD13^-$ proliferating cells, suggesting the significance of dormancy as an essential protective mechanism of therapy resistance. However, this mechanism may also play a role in the generation and accumulation of heterogeneity during cancer progression, although the exact mechanism remains to be understood. Through transcriptomic study, we elucidated the underlying epigenetic mechanism for malignant behavior of dormant CSCs, i.e., simultaneous activation of several pathways including EZH2- and TP53-related proteins in response to microRNA101, suggesting that a pharmacogenomic approach would open an era to novel molecular targeting cancer therapy.

Introduction

Recent studies have revealed that cancer stem cells (CSCs) are a source of therapy resistance, disease recurrence, and metastasis to other organs (1-3). At least two types of CSCs, dormant (dCSC) and activated (aCSC), are involved in tumor homeostasis, which are in contrast to two types of stem cells, dormant and activated types in normal skin, intestine and the hematopoietic system (4). Our previous study indicated that $CD13^+CD90^-$ dCSCs of hepatocellular carcinoma survive in hypoxic areas in marginal regions in liver after therapy (5). In $CD13^+/CD90^-$ dCSCs, the occurrence of double-strand breaks (DSBs) in genomic DNA, a deleterious cellular event, and damage-induced repairs that are necessary for cellular survival (6), reduce after therapy presumably due to CD13/aminopeptidase N functioning as a scavenger of reactive oxygen species (ROS) (5) and partially due to error-prone repair such as non-homologous end-joining (NHEJ) (6,7). In a sharp contrast, $CD13^-/CD90^{+/-}$ dCSCs are sensitive to therapeutic insults from chemotherapeutic agents, which is associated with ROS-induced cell death after chemotherapy (8); however, damage is typically repaired though high-fidelity, error-free homologous recombination (HR) (6,7). Thus, dCSCs may be a cause of accumulation of deleterious mutations and should be targeted in therapy in terms of complete eradication of malignant cells, although hibernation therapy (the induction of dormancy) may be a viable option dependent on the patient's condition (7). Chemotherapy results in a shift from aCSCs to dCSCs and accumulation of dCSCs after treatment, and dormancy may function as a type of refuge for the survival of malignant cells. CD13 cells play a role in the inhibition of increase in ROS and the resultant suppression of cell death during the process of epithelial mesenchymal transition (EMT) of metastatic CSCs (9). The exposure to a CSC-specific inhibitor, ubenimex, resulted in considerable eradication of malignant cells *in vivo*, indicating an apparent benefit in the combination of conventional chemotherapy and a CSC-specific inhibitor.

Here, we performed transcriptome analysis for coding mRNAs and non-coding microRNAs (miRs) in $CD13^+/CD90^-$ dCSCs. This study allowed us to identify several pathways, which play a role in fundamental mechanisms in above-mentioned potentially malignant phenotype, and provided further clues for identification of molecular targets in therapeutic approaches for dCSCs.

Materials and methods

Cell cultures. Cell lines were maintained in Dulbecco's modified Eagle's medium (DMEM; Nacalai Tesque, Kyoto, Japan)

Correspondence to: Dr Masaki Mori, Department of Gastroenterological Surgery, Osaka University, Graduate School of Medicine, Suita, Yamadaoka 2-2, Osaka 565-0871, Japan
E-mail: mmori@gesurg.med.osaka-u.ac.jp

Professor Hideshi Ishii, Department of Frontier Science for Cancer and Chemotherapy, Osaka University, Graduate School of Medicine, Suita, Yamadaoka 2-2, Osaka 565-0871, Japan
E-mail: hishii@cfs.med.osaka-u.ac.jp

Key words: transcriptome, cancer stem cells, dormancy, chemotherapy

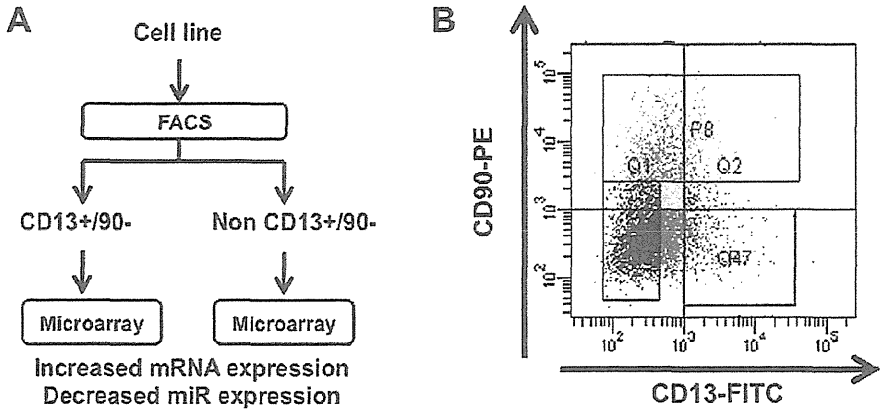

Figure 1. Isolation and analysis of liver dCSCs. (A) Cells were separated by FACS into dCSCs ($CD13^+/CD90^-$) and non-dCSCs ($CD13^+/CD90^+$, $CD13^-/CD90^+$, and $CD13^-/CD90^-$). Total-RNA was extracted and subjected to array screening for mRNA and miR. Here we focused on increased mRNA expression and decreased miR expression. (B) Representative data of FACS separation and sorting.

supplemented with 10% fetal bovine serum (FBS) at 37°C in a 5% humidified CO_2 atmosphere.

Flow cytometric analysis and cell sorting. The antibodies used were purchased from BD Biosciences (Tokyo, Japan). In brief, cells were harvested with trypsin and EDTA. Doublet cells were eliminated using FSC-A/FSC-H and SSC-A/SSC-H. Dead and dying cells were eliminated with 7-AAD (BD Pharmingen, San Jose, CA, USA). Isotype controls (BD Biosciences) were used. FcR blocking was performed using an FcR blocking reagent (Miltenyi Biotec, Bergisch Gladbach, Germany).

RNA. Total-RNA was extracted using TRIzol reagent (Invitrogen/Life Technologies Japan, Tokyo, Japan). Reverse transcription was performed with SuperScript III reverse transcription kit (Invitrogen). qPCR was performed using the LightCycler TaqMan Master Kit (Roche Diagnostics, Tokyo, Japan) for cDNA amplification of target-specific genes. Purified cDNA from mouse ES cells was used as a positive control for target genes. The expression of mRNA copies was normalized to GAPDH (for mRNA) or RNU48 (for miR) expression, as indicated. The RNA samples were analyzed using SurePrint G3 Human GE 8x60K Microarray and the Human miRNA Microarray 8x15K Rel.12.0 (Takara, Kyoto, Japan).

Statistical analysis. For continuous variables, results are expressed as means ± SE. The relationship between the gene expression level and cell count was analyzed by chi-square and Wilcoxon rank tests. All data were analyzed using JMP software (SAS Institute, Cary, NC, USA). P-values of <0.05 were considered statistically significant.

Results and Discussion

A study of $CD13^+/CD90^-$ as dCSCs. $CD13^+$/aminopeptidase N is expressed in liver CSCs (5), where it is involved in the reduction of ROS through the glutathione reductase pathway. Considering that another independent study has shown $CD90^+$ as a candidate stem marker, critical to tumorigenicity in mice *in vivo* and clinical outcomes of patients (10), we indicated that $CD13^+/CD90^-$ cells exist in dormant phase of cell cycle, whereas $CD13^+/CD90^+$ cells are predominantly in the S phase and $CD13^-/CD90^+$ cells are in the G2/M phase (5). In previous studies, we have elucidated that following exposure to genotoxic insults, such as chemotherapy or radiation therapy, $CD13^-$ cells shift to the $CD13^+$ fraction in dormant phase of cell cycle. In dCSCs, double stranded breaks (DSBs) are repaired predominantly through the error-prone NHEJ mechanism (6,7). In sharp contrast, the high-fidelity HR-type repair proteins are increased in non-dormant CSCs compared with NHEJ proteins, of which cells are usually sensitized through chemoradiation therapy (6,7). Thus, after chemoradiation therapy, NHEJ supposedly contributes to the generation of misrepair after DSBs, which may cause chromosomal deletions, insertions, or translocations, and subsequent genomic instability (11). Such genomic alterations lead to the inactivation of tumor suppressor genes and activation of oncogenes, which become more apparent during tumor development of primary lesions, recurrence and metastasis (12). Nevertheless, there remains an important issue to be addressed, i.e., the identification of molecular mechanisms fundamental for initiation and development of tumor tissues composed of stem cell hierarchy, and moreover, the type of mechanism involved in CSC-based heterogeneous tumors. We began with transcriptome assessment, i.e., the expression of mRNAs and miRs and their association with $CD13^+/CD90^-$ cells in supporting or maintaining CSC survival in the absence of genotoxic stimuli, which may be beneficial in the study of the basal situation and may help understand the differences between therapy-resistant clones and *de novo* tumor-initiating cells.

As shown in Fig. 1, we separated liver cancer cells by FACS sorting into $CD13^+CD90^-$ dCSCs from other non-CSCs. Considering that miRs play a role in the regulation of mRNA in its stability and translation as an inhibitory regulation system, we focused on increased expression of mRNA clones and decreased expression of miR clones. The data of high-density array screening indicated 17 clones of increased expression in $CD13^+CD90^-$ populations compared with unsorted cells with more than 2-fold significant increase. The data were almost consistent in $CD13^+/CD90^-$ populations

Table I. mRNAs expressed highly in CD13$^+$CD90$^-$ PLC cells.

mRNA	CD13$^+$CD90$^-$/ unsorted	CD13$^+$CD90$^-$/ non-CD13$^+$CD90$^-$
Cadherin 6, type 2, K-cadherin (CDH6)	3.33	3.21
Interleukin 8 (IL8)	3.27	1.50
Aldehyde dehydrogenase 1 family, member A3 (ALDH1A3)	3.26	2.61
Endothelin 1 (EDN1)	3.20	1.16
Cytochrome P450, family 1, subfamily B, polypeptide 1 (CYP1B1)	3.16	2.06
Tumor necrosis factor, α-induced protein 6 (TNFAIP6)	3.13	1.83
Chemokine (C-X-C motif) ligand 1 (CXCL1)	3.08	1.25
Vascular cell adhesion molecule 1 (VCAM1)	2.94	2.49
L1 cell adhesion molecule (L1CAM)	2.72	2.40
Wingless-type MMTV integration site family member 2 (WNT2)	2.66	1.10
Carcinoembryonic antigen-related cell adhesion molecule 3 (CEACAM3)	2.65	1.99
Chemokine (C-X-C motif) ligand 3 (CXCL3)	2.29	1.79
Chemokine (C-C motif) ligand 20 (CCL20)	2.24	2.44
Chemokine (C-X-C motif) ligand 12 (CXCL12)	2.11	1.53
Tumor necrosis factor (TNF superfamily, member 2) (TNF)	2.07	1.59
Chemokine (C-X-C motif) ligand 5 (CXCL5)	2.04	1.52
Wingless-type MMTV integration site family, member 7B (WNT7B)	2.02	1.16

The relative expressions in CD13$^+$CD90$^-$ PLC cells are shown as the ratio to unsorted, or to excluded populations (non CD13$^+$CD90$^-$).

Table II. miRs expressed highly in CD13$^+$CD90$^-$ PLC cells.

miR	CD13$^+$CD90$^-$/ unsorted	Non CD13$^+$CD90$^-$/ unsorted	Function
hsa-miR-374a	-8.24	0.19	Downregulated upon cisplatin exposure
hsa-miR-489	-7.17	0.41	miR-489 inhibited cell growth in all head and neck cancer cell lines
hsa-miR-223	-6.69	0.16	Reduced miR-223 expression in primary MEF leads to increased Fbw7 expression and decreased cyclin-E activity
hsa-miR-101	-6.68	-0.21	miR-101 could sensitize hepatoma cell lines to both serum starvation- and chemotherapeutic drug-induced apoptosis. Genomic loss of miR 101 leads to overexpression of histone methyltransferase EZH2 in cancer
hsa-miR-9	-6.29	0.70	Directly repress Lin28
hsa-miR-378	-6.21	-0.06	Novel target of the c-Myc oncoprotein that is able to cooperate with activated Ras or HER2 to promote cellular transformation
hsa-miR-182	-6.14	-0.68	Antagonizing miR-182 enhances BRCA1 protein levels and protects them from IR-induced cell death
hsa-miR-421	-5.69	0.20	Overexpression of miR-421 in pancreatic cancer cells promoted cell proliferation and colony formation
hsa-miR-125a-3p	-4.99	0.01	Hypoxia regulated microRNA

The relative expressions in CD13$^+$CD90$^-$ PLC cells are shown as the ratio to unsorted, or to excluded populations (non CD13$^+$CD90$^-$).

compared with non-CD13$^+$/CD90$^-$ cells (Table I). Next, we analyzed miR expression and successfully isolated nine miRs in CD13$^+$/CD90$^-$ population compared with unsorted cells with more than 4-fold significant decrease. The data were almost consistent in CD13$^+$/CD90$^-$ populations compared with non-CD13$^+$/CD90$^-$ cells (Table II).

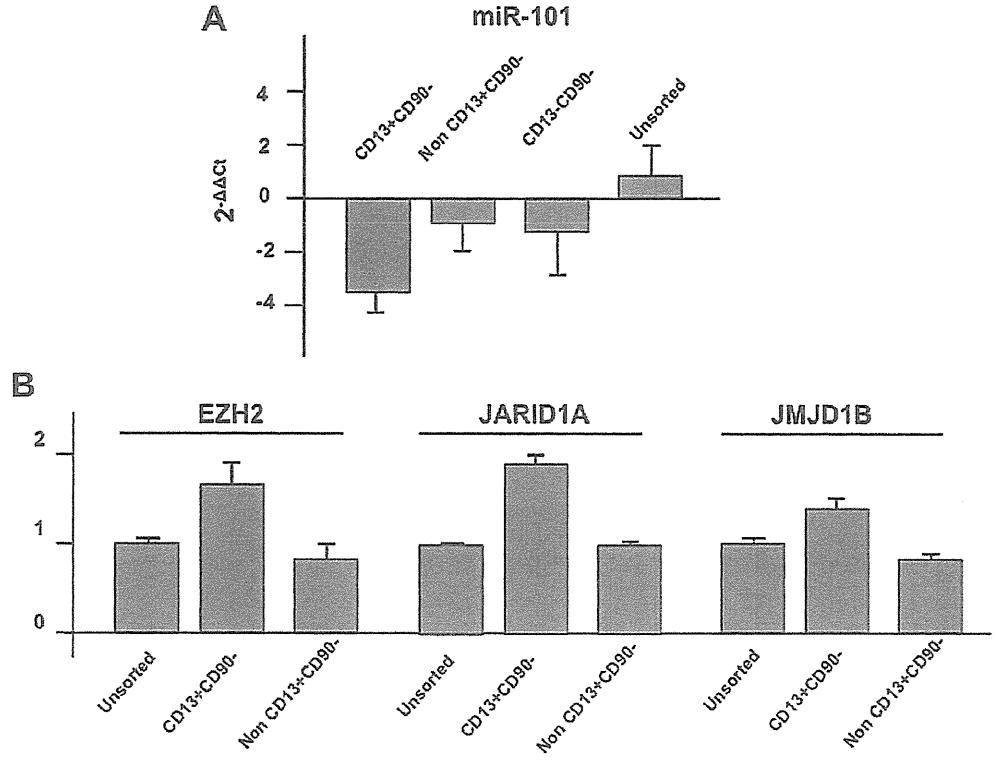

Figure 2. Quantitative analysis of isolated mRNA and miR transcripts by RT-PCR. RNAs from cells were extracted and subjected to qRT-PCR. Data of (A) miR study and (B) mRNA study are shown.

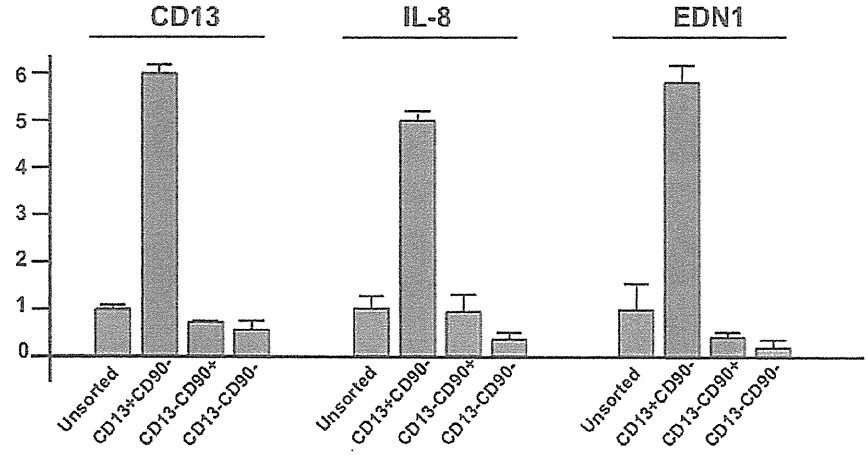

Figure 3. Quantitative analysis of isolated mRNA and miR transcripts by RT-PCR. RNAs from cells were extracted and subjected to qRT-PCR. Data of mRNA study are shown.

Identification of regulatory networks. By assessment of pairs of miRs and its putative target mRNAs using prediction software (http://www.targetscan.org/; http://www.microrna.org/microrna/home.do), we confirmed the data of the array by quantitative PCR. As shown in the representative data, the expression of miR-101 was downregulated in $CD13^+/CD90^-$ cells compared with non-$CD13^+/CD90^-$ cells or $CD13^-/CD90^-$ cells; in sharp contrast, the expression of putative targets, EZH2 (enhancer of zeste homolog 2; http://www.genecards.org/cgi-bin/carddisp.pl?gene=EZH2&search = EZH2), JARID1A; (http://www.genecards.org/cgi-bin/carddisp.pl?gene =KDM5A&search=JARID1A), and JMJD1B (http://www.genecards.org/cgi-bin/carddisp.pl?gene=KDM3B&search=JMJD1B) were increased (Fig. 2; summarized in Fig. 3). CD13 mRNA expression was increased in $CD13^+/CD90^-$ cells, but not in $CD13^-/CD90^+$, $CD13^-/CD90^-$, or unsorted cells. The expression of interleukin-8 (IL-8; http://www.genecards.org/cgi-bin/carddisp.pl?gene=IL8&search=Interleukin+8) and endothelin 1 (EDN1; http://www.genecards.org/cgi-bin/carddisp.pl?gene=EDN1&search=Endothelin+1) was increased in

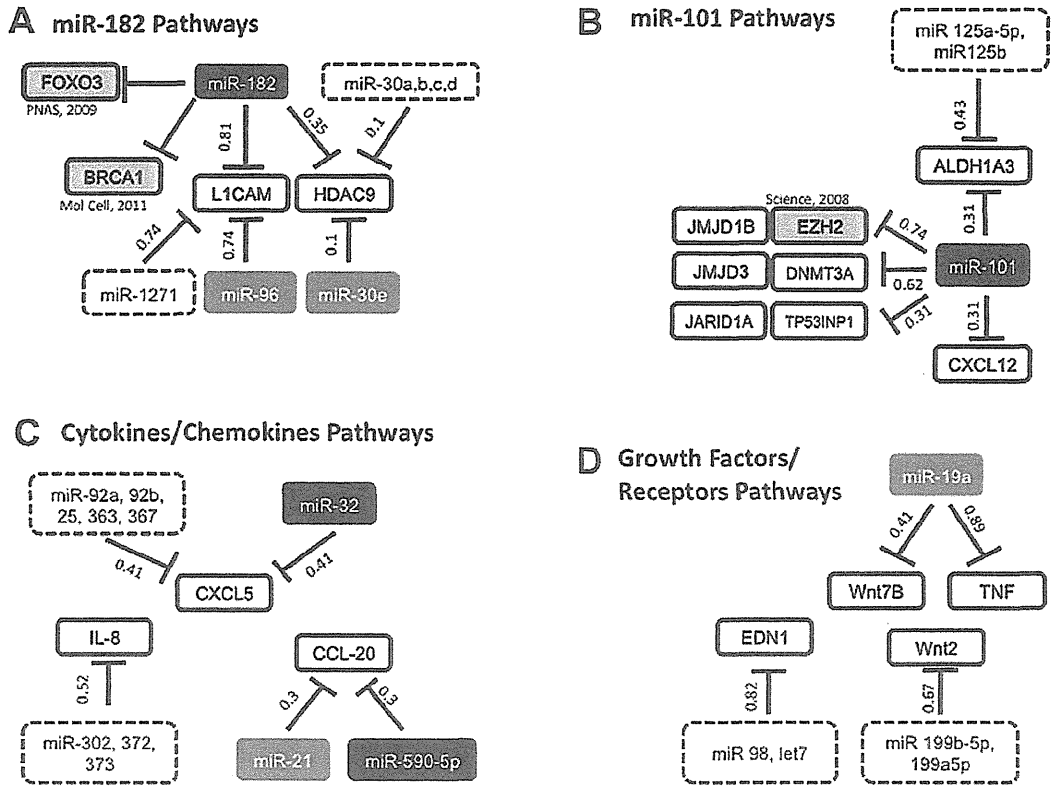

Figure 4. Summary of identified networks. The present study identified several networks, i.e., (A) miR-182 pathways, (B) miR-101 pathways, (C) cytokine/chemokine pathways and (D) growth factors and their receptor pathways. Closed characters in black (mir-101, mir-182, miR-32 and miR-590-5p) indicate identified and verified molecules in this study, whereas closed characters in gray (miR-96, miR-30e, miR21, miR019a) show molecules of which significance was already suggested in previous studies (3,25). Closed characters by dashed lines indicate molecules that were not verified in this study as linked to $CD13^+/CD90^-$ dormancy. As target mRNAs, closed characters in gray (FOXO3, BRCA1 and EZH2, and miR-182) indicate identified and verified molecules in this study and already reported as significant in previous publications, whereas open characters in bold (LICAM, HDAC9, JMJD1B, JMJD3, DNMT3A, JARID1A, TP32INP1, ALDH1A3, CXCL12, CXCL5, IL-8, CCL-20, Wnt7B, TNF, EDN1 and Wnt2) denote novel unpublished molecules identified and verified in this study.

$CD13^+/CD90^-$ cells, but not in others (Fig. 3; summarized in Fig. 3). Through this study, we were able to find at least three core regulatory networks for the maintenance of dormant $CD13^+/CD90^-$ cells, but not in others, i.e., miR-182 pathways, miR-101 pathways, cytokines/chemokines pathways (IL-8, CXCL5 [http://www.genecards.org/cgi-bin/carddisp.pl?gene=CXCL5&search=CXCL5], CCL-20 [http://www.genecards.org/cgi-bin/carddisp.pl?gene=CCL20& search=CCL-20]), growth factors and their receptor pathways [EDN1, Wnt2 (http://www.genecards.org/cgi-bin/carddisp.pl?gene=WNT2&search=Wnt2), Wnt7B (http://www.genecards.org/cgi-bin/carddisp.pl?gene=WNT7B&search = Wnt7B), and TNF (http://www.genecards.org/cgi-bin/carddisp.pl?gene =TNF&search=TNF)]. As noted in this study, we did not detect any apparent involvement in DNA damage response machineries, except for an association underlined by TP53INP1 (http://www.genecards.org/cgi-bin/carddisp.pl?gene=TP53INP1&search =TP53INP1) and BRCA1 (http://www.genecards.org/cgi-bin/carddisp.pl?gene=BRCA1& search = BRCA1), suggesting that (1) the damage response in dCSCs is characteristic after exposure to genotoxic stimuli, whereas in the absence of damage insults, they are not apparent and (2) the DNA damage response was regulated mainly by the modification of proteins such as phosphorylation or ubiquitination, and the expression array technology was less sensitive to pathway detection and other networks may have been missed.

Significance of regulatory networks (Fig. 4). The EZH2 gene encodes a member of the Polycomb group (PcG) family, which forms multimeric protein complexes involved in maintaining a transcriptionally repressive state of genes over successive cellular generations (13). Reportedly, the genomic loss of miR-101, a putative tumor suppressor, leads to overexpression of histone methyltransferase EZH2 in cancer (14,15), hypoxia, and androgen-dependent conditions (16) as well as in gastric cancer (17), pancreatic cancer (18), lung cancer (19) glioblastoma (20) and invasive squamous cell carcinoma (21). Thus, PcG proteins are critical epigenetic mediators of stem cell pluripotency and CSC functions, which may be implicated in human cancer pathogenesis, probably indicating candidacy for novel pharmacological targets of cancer therapy. Recently, it was reported that the administration of diflourinated-curcumin (CDF), a novel analogue of the turmeric spice component curcumin, has antioxidant properties and inhibits tumor growth through reduced expression of EZH2, Notch-1, CD44, EpCAM, and Nanog and increased expression of let-7, miR-26a, and miR-101 (18). These findings indicated that CDF inhibited CSC growth by targeting an EZH2-miRNA regulatory circuit for epigenetically controlled gene expression. In the present study,

we identified various miR-101 targets, including JARID1A, JMJD1B, TP53INP1, and EZH2, suggesting that these target molecules act together to maintain CSC dormancy, and proposed the possible significance of the miR-101 pathway. We also identified the miR-182 pathway, in which miR-182-mediated downregulation of BRCA1 impacts DNA repair and sensitivity to poly-ADP ribose polymerase (PARP) inhibitors (22). The overexpression of miR-182 was reported in high-grade ovarian papillary serous carcinoma (23). Reportedly, aberrant miR-182 expression promotes melanoma metastasis by repressing FOXO3 (24). Taken together with our study, the miR-182 pathway may be involved in the maintenance of CSC function in a similar manner. As summarized in Fig. 4, we identified other cytokines, chemokines, growth factors, receptors and pathways. These findings may facilitate further studies on the regulatory mechanisms of the dormant phase of gastrointestinal CSCs.

References

1. Reya T, Morrison SJ, Clarke MF and Weissman IL: Stem cells, cancer, and cancer stem cells. Nature 414: 105-111, 2001.
2. Visvader JE and Lindeman GJ: Cancer stem cells in solid tumours: accumulating evidence and unresolved questions. Nat Rev Cancer 10: 755-768, 2008.
3. Dewi DL, Ishii H, Kano Y, *et al*: Cancer stem cell theory in gastrointestinal malignancies: recent progress and upcoming challenges. J Gastroenterol 46: 1145-1157, 2011.
4. Li L and Clevers H: Coexistence of quiescent and active adult stem cells in mammals. Science 327: 542-545, 2010.
5. Haraguchi N, Ishii H, Mimori K, *et al*: CD13 is a therapeutic target in human liver cancer stem cells. J Clin Invest 120: 3326-3339, 2010.
6. Sancar A, Lindsey-Boltz LA, Unsal-Kacmaz K and Linn S: Molecular mechanisms of mammalian DNA repair and the DNA damage checkpoints. Annu Rev Biochem 73: 39-85, 2004.
7. Nishikawa S, Ishii H, Haraguchi N, *et al*: Genotoxic therapy stimulates error-prone DNA repair in dormant hepatocellular cancer stem cells. Exp Ther Med (In press).
8. Haraguchi N, Ishii H, Nagano H, Doki Y and Mori M: The future prospects and subject of the liver cancer stem cells study for the clinical application. Gastroenterology: Feb 23, 2011 (Epub ahead of print).
9. Kim HM, Haraguchi N, Ishii H, *et al*: Increased CD13 expression reduces reactive oxygen species, promoting survival of liver cancer stem cells via an epithelial-mesenchymal transition-like phenomenon. Ann Surg Oncol: Aug 31, 2011 (Epub ahead of print).
10. Yang ZF, Ho DW, Ng MN, *et al*: Significance of $CD90^+$ cancer stem cells in human liver cancer. Cancer Cell 13: 153-166, 2008.
11. Weinstock DM, Richardson CA, Elliott B and Jasin M: Modeling oncogenic translocations: distinct roles for double-strand break repair pathways in translocation formation in mammalian cells. DNA Repair (Amst) 5: 1065-1074, 2006.
12. Ishii H, Iwatsuki M, Ieta K, Ohta D, Haraguchi N, Mimori K and Mori M: Cancer stem cells and chemoradiation resistance. Cancer Sci 99: 1871-1877, 2008.
13. Chen H, Rossier C and Antonarakis SE: Cloning of a human homolog of the Drosophila enhancer of zeste gene (EZH2) that maps to chromosome 21q22.2. Genomics 38: 30-37, 1996.
14. Varambally S, Cao Q, Mani RS, *et al*: Genomic loss of microRNA-101 leads to overexpression of histone methyltransferase EZH2 in cancer. Science 322: 1695-1699, 2008.
15. Friedman JM, Liang G, Liu CC, *et al*: The putative tumor suppressor microRNA-101 modulates the cancer epigenome by repressing the polycomb group protein EZH2. Cancer Res 69: 2623-2629, 2009.
16. Cao P, Deng Z, Wan M, Huang W, *et al*: MicroRNA-101 negatively regulates Ezh2 and its expression is modulated by androgen receptor and HIF-1alpha/HIF-1beta. Mol Cancer 9: 108, 2010.
17. Wang HJ, Ruan HJ, He XJ, *et al*: MicroRNA-101 is down-regulated in gastric cancer and involved in cell migration and invasion. Eur J Cancer 46: 2295-2303, 2010.
18. Bao B, Ali S, Banerjee S, Wang Z, *et al*: Curcumin analogue CDF inhibits pancreatic tumor growth by switching on suppressor microRNAs and attenuating EZH2 expression. Cancer Res 72: 335-345, 2012.
19. Zhang JG, Guo JF, Liu DL, Liu Q and Wang JJ: MicroRNA-101 exerts tumor-suppressive functions in non-small cell lung cancer through directly targeting enhancer of zeste homolog 2. J Thorac Oncol 6: 671-678, 2011.
20. Smits M, Nilsson J, Mir SE, *et al*: miR-101 is down-regulated in glioblastoma resulting in EZH2-induced proliferation, migration, and angiogenesis. Oncotarget 1: 710-720, 2010.
21. Banerjee R, Mani RS, Russo N, *et al*: The tumor suppressor gene rap1GAP is silenced by miR-101-mediated EZH2 overexpression in invasive squamous cell carcinoma. Oncogene 30: 4339-4349, 2011.
22. Moskwa P, Buffa FM, Pan Y, *et al*: miR-182-mediated downregulation of BRCA1 impacts DNA repair and sensitivity to PARP inhibitors. Mol Cell 41: 210-220, 2011.
23. Liu Z, Liu J, Segura MF, *et al*: MiR182 overexpression in tumorigenesis of high-grade ovarian papillary serous carcinoma. J Pathol: Feb 9, 2012 (Epub ahead of print).
24. Segura MF, Hanniford D, Menendez S, *et al*: Aberrant miR-182 expression promotes melanoma metastasis by repressing FOXO3 and microphthalmia-associated transcription factor. Proc Natl Acad Sci USA 106: 1814-1819, 2009.
25. Dewi DL, Ishii H, Haraguchi N, *et al*: Reprogramming of gastrointestinal cancer cells. Cancer Sci 103: 393-399, 2012.

Ann Surg Oncol (2012) 19:1357–1364
DOI 10.1245/s10434-011-1739-7

Annals of
SURGICAL ONCOLOGY
OFFICIAL JOURNAL OF THE SOCIETY OF SURGICAL ONCOLOGY

ORIGINAL ARTICLE – TRANSLATIONAL RESEARCH AND BIOMARKERS

Absence of CD71 Transferrin Receptor Characterizes Human Gastric Adenosquamous Carcinoma Stem Cells

Masahisa Ohkuma, MD[1,2], Naotsugu Haraguchi, MD, PhD[1], Hideshi Ishii, MD, PhD[1,3], Koshi Mimori, MD, PhD[3], Fumiaki Tanaka, MD, PhD[3], Ho Min Kim, MD[1], Miho Shimomura, MD[1], Hajime Hirose, MD[1], Katsuhiko Yanaga, MD, PhD[2], and Masaki Mori, MD, PhD[1]

[1]Department of Gastroenterological Surgery, Graduate School of Medicine, Osaka University, Osaka, Japan; [2]Department of Surgery, Jikei University School of Medicine, Tokyo, Japan; [3]Department of Surgery, Medical Institute of Bioregulation, Kyushu University, Oita, Japan

ABSTRACT

Background. Although the importance of cancer stem cells (CSCs) in overcoming resistance to therapy and metastasis has recently been reported, the role of CSCs in gastric cancer remains to be elucidated.

Methods. MKN-1 cells were used to study markers of CSCs in gastric adenosquamous carcinoma, as these cells are suitable for determining multidifferentiation ability. Changes in expression of CD44, CD49f, CD133, and CD71 following 5-fluorouracil (5-FU) treatment were assessed.

Results. After 5-FU treatment, only the $CD71^-$ fraction was significantly increased. Investigation of CD71 indicated that the $CD71^-$ cell fraction was present in the G1/G0 cell cycle phase and showed high resistance to the anticancer agent 5-FU. Limiting dilution and serial transplantation assays revealed the $CD71^-$ cell fraction to have higher tumorigenicity than the $CD71^+$ cell fraction. The $CD71^-$ cell fraction showed multipotency to adenocarcinoma and squamous cell carcinoma. A three-dimensional (3D) invasion assay and immunohistochemical analysis showed $CD71^-$ cells to be highly invasive and to exist in the invasive fronts of cancer foci.

Conclusion. The present study suggests that use of $CD71^-$ as a marker for adenosquamous carcinoma may provide a useful model for studying CSCs.

First Received: 9 September 2010;
Published Online: 27 April 2011

H. Ishii, MD, PhD
e-mail: hishii@gesurg.med.osaka-u.ac.jp

M. Mori, MD, PhD
e-mail: mmori@gesurg.med.osaka-u.ac.jp

Recent studies have identified a small fraction of cancer stem cells (CSCs) that are capable of self-renewal and multipotency and play a role in tumor progression.[1–4] Although "total cell kill therapy" reduces tumor size, the malignant cells that survive are believed to include CSCs, resulting in clinically important consequences such as metastasis, relapse, and resistance to therapy.[1–4] Gastric cancer is relatively common in East Asia and South America. It is the fourth most frequently diagnosed malignant tumor in the world and the second most lethal disease after lung cancer.[5] There are few implications for the markers of CSCs in gastric cancer except CD44 and side population (SP) cells.[6,7] To the best of our knowledge, to date no report has focused on the multipotency of gastric cancer CSCs. Although adenosquamous carcinoma is believed to represent less than 1% of all gastric cancers, it is a good model for understanding the mechanism underlying the multipotency of CSCs as well as cellular hierarchy.

MATERIALS AND METHODS

Cell Preparation and Culture

MKN-1 cells were obtained from the Japanese Collection of Research Bioresources Cell Bank. Cells were cultured in Roswell Park Memorial Institute (RPMI) 1640 medium (Invitrogen)/10% fetal bovine serum (FBS) containing 100 μg/ml penicillin G and 100 units/ml streptomycin at 37°C in 5% CO_2 atmosphere. Four samples of human gastric adenosquamous carcinoma were obtained from Kyushu University in Japan with the approval of the Research Ethics Board at the university and the informed consent of the patients. To obtain tumor cells from xenografted mice, tumors were digested with 2 mg/ml collagenase A (Roche Diagnostics) solution.

Flow Cytometry Analysis

After FcR blocking (Miltenyi Biotec), cells were stained with the following anti-human antibodies: phycoerythrin (PE)-CD71 (BD Biosciences), allophycocyanin (APC)-CD133/1 (Miltenyi Biotec), PE-CD44 (BD Pharmingen), and PE-CD49f (BD Pharmingen), and isotype control antibody (BD Biosciences). After doublet cell elimination, dead cells were eliminated using 7-amino actinomycin D. FACSVantage SE DiVa (Becton Dickinson) and FACS SORP Aria (Becton Dickinson) were used for analysis and cell sorting. To isolate human cells from mouse xenografts, biotinylated anti-mouse H-2Kd (BD Pharmingen) and biotinylated anti-mouse CD45 (BD Pharmingen) antibodies were used. Streptavidin-APC-Cy7 (BD Pharmingen) was used as the secondary antibody.

Cell Cycle Assay

To characterize SP fractions, 1×10^6 cells were labeled with 10 μg/ml Hoechst 33342 (Invitrogen) in a staining medium at 37°C for 70 min alone or with 50 μM Fumitremorgin C (Sigma-Aldrich). For cell cycle assays, cells were labeled with Hoechst 33342 (Invitrogen) at concentration of 5–10 μg/ml for 60–90 min at 37°C. Data were analyzed using Diva software (Becton Dickinson) and FlowJo software version 7.2 (Tree Star Inc.).

Colony Formation Assay

Cells were plated at density of 500–1,000 cells/well in three 35-mm plates (BD Falcon) and were stained on day 14 using the Diff-Quik kit (Sysmex Corp.).

Cell Proliferation Assay

Cell proliferation was examined on days 1, 3, 5, 7, and 9. Isolated cells were seeded into 96-well culture plates at 1×10^3 cells/well. After 72 h, cell viability was determined by an adenosine triphosphate (ATP) bioluminescence assay (CellTiter-Glo Luminescent Cell Viability Assay; Promega). Luminescence signals were detected using a luminometer (VICTOR3 Multilabel Plate Counter, PerkinElmer).

Migration and Invasion Assays

For migration and invasion assays, the cells (2.5×10^4 cells/well) were placed in the upper chamber of a BD BioCoat tumor invasion system (Becton Dickinson), and the lower chamber was filled with a culture medium containing 10% FBS. The membranes were labeled using calcein AM solution after 72 h of incubation.

3D Culturing

After sorting, the cells were plated on 24-well plates coated with Matrigel (BD Biosciences) at density of 5×10^3/ml and cultured for 21 days in a medium that was changed every 72 h.

Transplantation of Cancer Cells

The isolated cells were resuspended in 1:1 mixture of medium and Matrigel (BD Biosciences) to final volume of 200 μl. Tumor cells were injected into the bilateral axillary fossa of 4-week-old female nonobese diabetic/severe combined immunodeficiency (NOD/SCID) mice under anesthesia. Eight weeks after inoculation, the grafts were removed for further studies.

Immunohistochemistry

Paraffin-embedded tissue sections were stained with anti-human MUC6 (Thermo Scientific), anti-human CK5/6 (DakoCytomation), and anti-human CD71 (Thermo Scientific) antibodies. Antibodies were detected using Envision reagents (EnVision + Dual Link System-HRP; DakoCytomation).

Statistical Analysis

For continuous variables, data are expressed as mean ± standard deviation (SD). Differences between groups were estimated by Student's *t*-test and repeated-measures analysis of variance (ANOVA). All differences were deemed significant at a level of $P < 0.05$.

RESULTS

Assessment of CSC Markers Using Anticancer Drugs

Previous reports have indicated that CSCs are resistant to chemotherapy.[1–4] Repeated exposure to anticancer drugs is believed to enhance the survival of CSCs while other daughter cells are inhibited, which leads to accumulation of the CSC fraction. Therefore, we assessed the response of MKN-1 cells on exposure to the anticancer drug 5-fluorouracil (5-FU) that is generally used in treating tumors of the digestive system.[8,9] After culturing MKN-1 cells in a growth medium with or without 5 μg/ml 5-FU for 7 days, changes in expression of cell surface markers were assessed. We evaluated CD44, CD49f, CD133, and CD71 as candidate markers; these have been reported as CSC markers for other organs or normal stem cells.[10–15] Following treatment with 5-FU, expressions of CD44, CD49f,

and CD133 were unaltered compared with those of the controls. On the other hand, the $CD71^-$ fraction increased from 18.6 to 82.0% after 5-FU treatment (Fig. 1). We then focused on the expression of CD71, because the $CD71^-$ fraction was enriched after 5-FU treatment.

Characterization of $CD71^-$ Cells In Vitro

As CSCs are typically characterized as capable of self-renewal, we studied their colony-forming capacity, which is assumed to reflect some aspects of self-reproduction.[1–4] The $CD71^-$ fraction showed profoundly higher colony-forming activity in vitro compared with that of the $CD71^+$ fraction (3.64-fold; $P < 0.05$; Fig. 2a).

Hematopoietic and leukemic stem cells exist in the G0/G1 cell cycle phase;[16–18] therefore, we examined the cell cycle status. Our data indicated that $CD71^-$ cells existed mainly in the G0/G1 phase (87.2 ± 2.53%), while $CD71^+$ cells existed mainly in the G2/M cell cycle phase (70.3 ± 5.61%; Fig. 2b).

To assess whether the $CD71^-$ cell population produced $CD71^+$ cells during cell proliferation, an isolated $CD71^-$ cell population was cultured to trace expression of CD71. The isolated $CD71^-$ cells rapidly produced $CD71^+$ cells within 1 week. The proportion of the $CD71^+$ cell fraction reached 80% in 10 days; the same percentage of the $CD71^+$ cell fraction was observed in the control MKN-1 cells. Conversely, the isolated and cultured $CD71^+$ cells produced a $CD71^-$ cell fraction of approximately 20% within 4 days of isolation. The proportion decreased to about 10% after 4 days (Fig. 2c). This was lower than the percentage of $CD71^-$ cells in the controls. $CD71^+$ and $CD71^-$ cells accounted for 81.4 and 18.6%, respectively, of control cells, suggesting that $CD71^+$ cells are less capable of producing $CD71^-$ cells.

Next, we assessed the scatter and invasive activities of sorted $CD71^+$ and $CD71^-$ cells. The scatter and invasive activities of $CD71^-$ cells were higher by 4.5- and 2.3-fold, respectively, than those of $CD71^+$ cells (Fig. 2d). To confirm the high cell migratory ability of $CD71^-$ cells, isolated $CD71^+$ and $CD71^-$ cells were seeded in a Matrigel-coated chamber and cultured for 21 days. Interestingly, $CD71^-$ cells formed spheroid-shaped and globular colonies, whereas $CD71^+$ cells formed small numbers of spheroid-shaped colonies, suggesting that $CD71^-$ cells possess high migratory and invasive potential (Fig. 2e).

As our data indicated that the $CD71^-$ population was resistant to 5-FU exposure, we considered the possibility that the drug exclusion activity of $CD71^-$ cells may be higher than that of $CD71^+$ cells. In the MKN-1 cell population, the percentage of the SP fraction was 5.8% (Fig. 2f), and 32.1% of the cells were $CD71^-$.

Tumorigenicity of $CD71^-$ Cells

To assess the tumorigenicity of $CD71^-$ and $CD71^+$ cells, isolated $CD71^+$ and $CD71^-$ cells were inoculated subcutaneously into NOD/SCID mice. Mice inoculated with 10,000, 5,000, and 2,500 $CD71^+$ or $CD71^-$ cells showed tumor formation after 8 weeks. Tumor initiation was more apparent among mice inoculated with 1,000 or 100 $CD71^-$ cells compared with mice inoculated with $CD71^+$ cells. In particular, when 100 cells were inoculated, all mice inoculated with the $CD71^-$ fraction developed

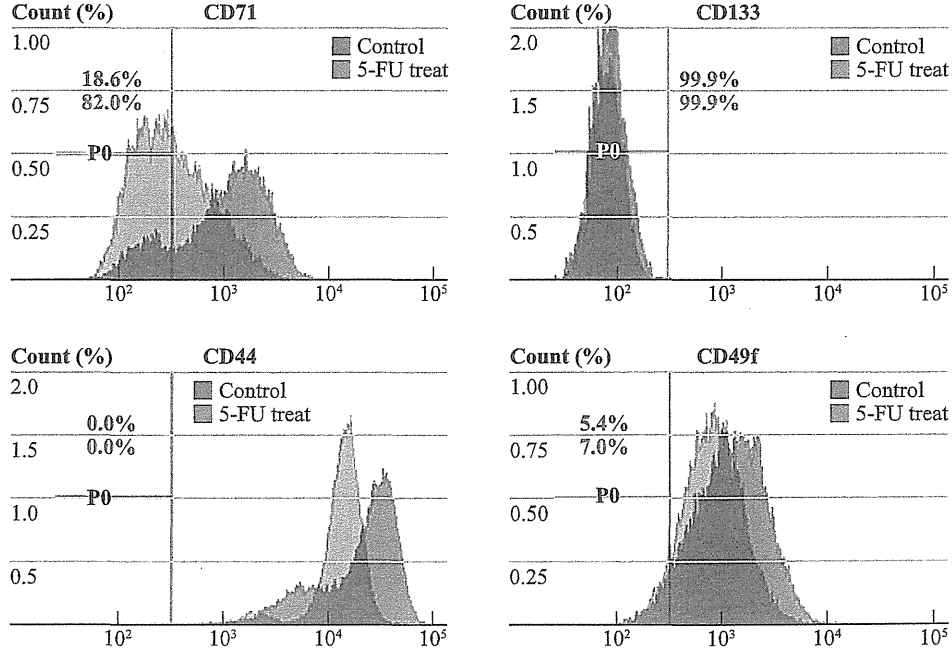

FIG. 1 $CD71^-$ cell fraction resistant to 5-FU treatment: Each panel displays the change in the CD71, CD133, CD44, and CD49f cell fractions after 5-FU treatment compared with controls. *Numbers* in each panel show the percentage of each negative cell fraction

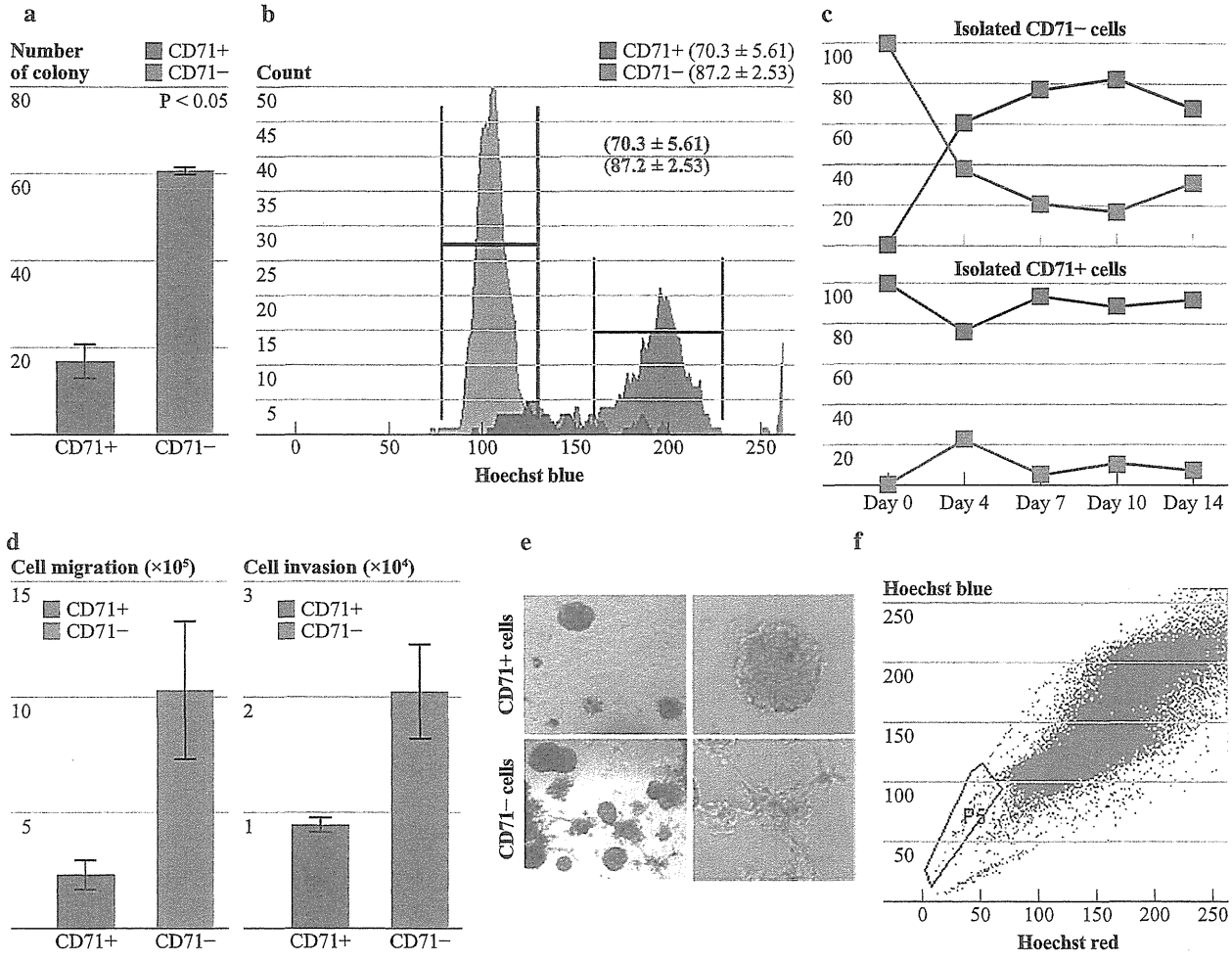

FIG. 2 $CD71^-$ cell fraction exists mainly in the G0/G1 cell cycle phase and shows high invasive ability: **a** Colony formation assay of isolated $CD71^-$ and $CD71^+$ cell fractions. Data are mean ± SD from independent experiments with differential fractions. $^*P < 0.05$. **b** Cell cycle assay of isolated $CD71^-$ and $CD71^+$ cell fractions. The number of the $CD71^-$ cell fraction (*red*) shows the percentage in G0/G1 cell cycle phase, and the number of the $CD71^+$ cell fraction (*blue*) shows the percentage in the G2/M cell cycle phase. **c** Time-course study of the changes in CD71 expression in isolated and cultured $CD71^-$ cells (*left*) and $CD71^+$ cells (*right*). **d** Cell migration (*left*) and invasive ability (*right*) of isolated $CD71^-$ and $CD71^+$ cell fractions. **e** 3D Matrigel culture of isolated $CD71^-$ and $CD71^+$ cell fractions. *Left column*, lower magnification (×10); *right column*, higher magnification (×20). *Bar* 100 μm. **f** Analysis of the SP fraction in MKN-1 cells

tumors (5/6, 83.3%), whereas none of the mice inoculated with the $CD71^+$ fraction developed tumors (0/6, 0%; Fig. 3a; Table 1). The size of the tumors formed was significantly larger in mice inoculated with 10,000, 1,000, and 100 $CD71^-$ cells than in mice inoculated with the $CD71^+$ fraction (Fig. 3b). Unfortunately, no metastatic lesions were observed in the $CD71^-$ and $CD71^+$ fraction-inoculated mice.

To assess tumorigenesis more definitively, a serial transplantation assay was performed. Similar to the results obtained with primary mice, the secondary mice developed tumors only after inoculation with 100 $CD71^-$ cells (3/5, 60%; Table 1; Fig. 3c). Tumorigenicity was relatively less than that in the primary mice, although the difference was apparent.

To assess whether $CD71^-$ cells produce $CD71^+$ cells in vivo, the tumors of $CD71^-$ cell-inoculated mice were digested to single cells and analyzed by flow cytometry. The data indicated that $CD71^-$ cell-derived tumors contained 21.6% $CD71^+$ cells, suggesting that $CD71^-$ cells produce $CD71^+$ cells (Fig. 3d). Interestingly, $CD71^+$ cell-derived tumors also contained $CD71^-$ cells (73.7%), suggesting that some part of the $CD71^+$ cell fraction produced $CD71^-$ cells (Fig. 3d).

Bipotentiality of CD71 Cells In Vivo

Histopathological examination revealed that tumor cells derived from isolated $CD71^-$ cells were heterogeneous with atypical nuclei and an apparently malignant

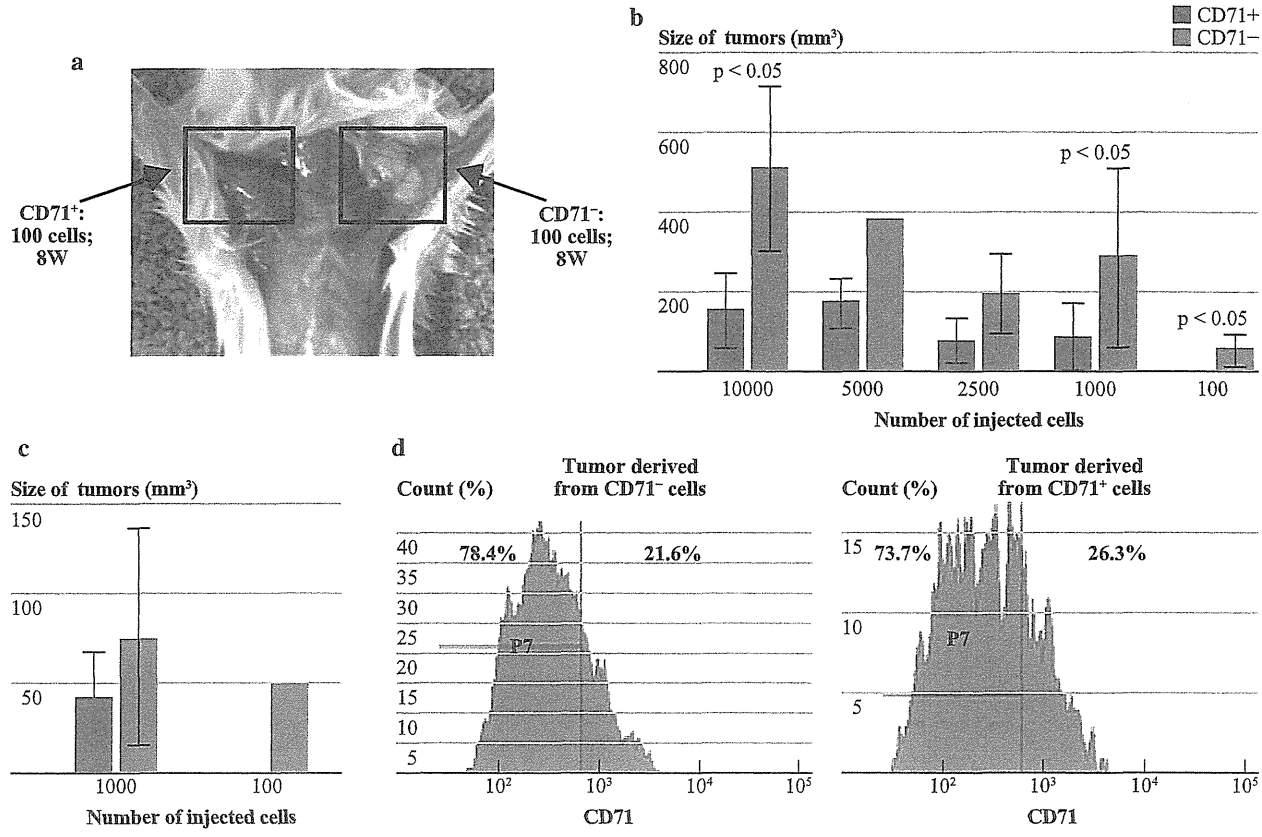

FIG. 3 $CD71^-$ cells have higher tumorigenicity: **a** Tumors formed from 100 isolated $CD71^-$ (*right solid square*) and $CD71^+$ (*left solid square*) fractions 8 weeks after inoculation into mice. **b** Tumor size derived from 10,000 to 100 isolated $CD71^-$ and $CD71^+$ cell fractions. Data are mean ± SD from independent experiments. $^*P < 0.05$. **c** Tumor size and tumor formation of serially transplanted $CD71^-$ and $CD71^+$ cell fractions. **d** Flow cytometry analysis of CD71 expression of digested tumors derived from $CD71^-$ (*upper*) and $CD71^+$ (*lower*) cell fractions

TABLE 1 Limiting dilution and serial transplantation assays of the $CD71^-$ and $CD71^+$ cell fractions

	Cell fraction	Numbers of injected cells				
		100	1,000	2,500	5,000	10,000
Limiting dilution	$CD71^-$	5/6	10/10	3/3	2/2	4/4
	$CD71^+$	0/6	8/10	3/3	3/3	5/5
Serial transplantation	$CD71^-$	3/5	5/5	–	–	–
	$CD71^+$	0/5	3/5	–	–	–

phenotype, whereas tumor cells from $CD71^+$ cells were not (Fig. 4a).

We used immunohistochemical staining to assess whether $CD71^-$ cells showed multipotency. Staining with anti-MUC6, a differentiation marker for adenocarcinoma, showed that tumors derived from $CD71^-$ and $CD71^+$ cells were positive for MUC6. In contrast, staining with anti-CK 5/6, a differentiation marker for the squamous cell lineage, demonstrated that tumors from all three $CD71^-$ cell-inoculated mice (100%) were strongly positive for CK 5/6, whereas all the tumors (3/3, 100%) obtained from $CD71^+$ cell-inoculated mice were completely negative for CK 5/6 (Fig. 4b). These findings suggest that $CD71^-$ cells produced adenocarcinoma and squamous cell carcinoma, whereas $CD71^+$ cells contributed predominantly to adenocarcinoma. Pathologically, the tumors derived from the $CD71^-$ fraction were very similar to those derived from the parent cells.

To confirm CD71 expression in clinical adenosquamous gastric cancer cases, specimens were stained with CD71 antibody. In all four samples, expression of CD71 was typically recognized in the main cancer foci as a cell surface molecule (Fig. 4c). In the present study, $CD71^-$ cells showed higher migratory and invasive ability than $CD71^+$ cells (Fig. 2d, e). Invasive fronts suggest a critical role in the progression and metastasis of tumors. Interestingly, in the present study, immunohistochemical analysis of human gastric adenosquamous carcinoma demonstrated that $CD71^-$ cells were distributed in whole tumors as well as in cluster formations at invasive fronts (Fig. 4c).

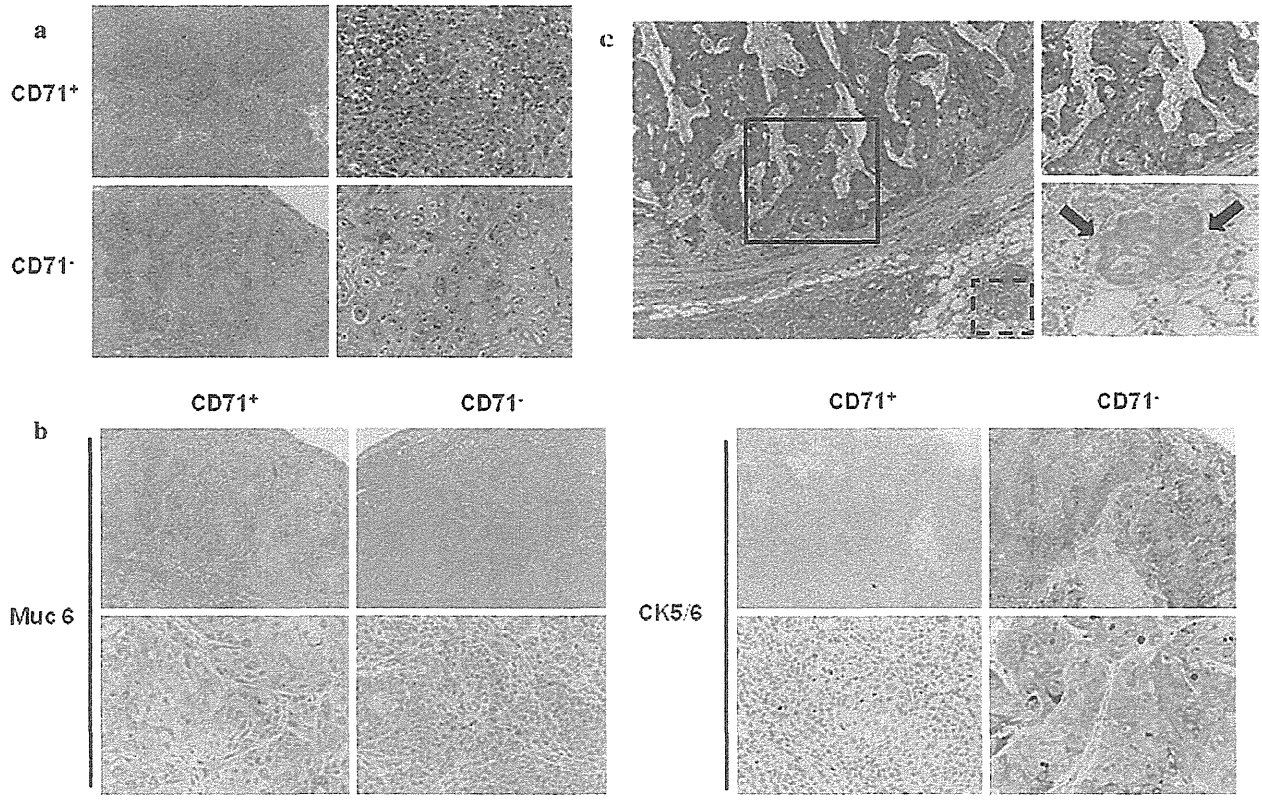

FIG. 4 CD71$^-$ cell fraction shows multipotency and exists in the invasive front of cancer foci: **a** Hematoxylin and eosin stain of tumor sections derived from isolated CD71$^-$ and CD71$^+$ cell fractions (*left*, ×10; *right*, ×20). **b** Immunohistochemical stains of tumor sections derived from isolated CD71$^-$ and CD71$^+$ cell fractions with anti-human MUC6 and anti-human CK 5/6 antibodies. Each of the *upper columns* shows the lower magnification (×10), and each *lower column* shows the higher magnification (×20). **c** Immunohistochemical stains with anti-human CD71 from a human gastric adenosquamous cancer specimen. The *left panel* shows the lower magnification (×10), and the *upper right panel* shows a higher magnification (×20) of the *solid square* in the *left panel*. The *lower right panel* shows a higher magnification (×20) of the invasive front of the cancer foci seen in the *dotted square* in the *left panel*

DISCUSSION

The significance of CSCs has become apparent over the past decade since the discovery of their importance in hematological malignancy.[19] CSCs are believed to play a key role in tumor relapse and metastasis. Increased knowledge of this role is expected to bring advances in cancer therapy, which has been limited until date.

In the present study, we identified the CD71$^-$ cell fraction as a potential multidifferentiation and high-tumorigenicity fraction in MKN-1 cells, which are a known cell line of gastric adenosquamous carcinoma. The CD71 transferrin receptor is a carrier protein that transports iron into the cell and maintains cellular iron homeostasis. Various stem cells have been reported to be CD71 diminished or negative, including hematopoietic, keratinocyte, and hair follicle bulge stem cells.[20–24] Malignant leukemic stem cells are also reported to be CD71$^-$.[25–28]

Multipotency is one of the important characters proving the stemness of CSCs. A marker that is useful for identifying a multipotential cell population will be a CSC marker. We studied CSCs using the MKN-1 cell line, a cell line derived from a very rare variant of adenosquamous carcinoma. CD44 and SP cells have been reported to be candidate markers of gastric cancer CSCs.[6,7] However, to the best of our knowledge, there has been no report that shows or identifies markers closely related to a multidifferentiation fraction. In the present study, staining with anti-MUC6, a differentiation marker for adenocarcinoma, and anti-CK 5/6, a differentiation marker for the squamous cell lineage, revealed that only tumors derived from CD71$^-$ cells contained MUC6- and CK 5/6-positive cells. This finding suggests the bilateral differentiation potential of CD71$^-$ cells into adenocarcinoma and squamous cell carcinoma. Histologically, the epithelial surface of the skin and esophagus are lined with squamous cells. As with keratinocyte stem cells, esophageal stem cells are reported to be CD71$^-$.[22,23,29,30] Although these reports are from studies of normal squamous stem cells, the fact that a squamous cell lineage can be derived from the CD71$^-$ cell

fraction may be relevant in the context of cancer. It is important to determine whether the squamous cell carcinoma and adenocarcinoma lineages can appear from a single cell.

The slow growth of CSCs partially contributes to their anticancer agent resistance and cancer recurrence after chemotherapy.[31] In leukemia, it has been reported that quiescent (existing in the G0 phase) leukemic CSCs survive after treatment with the common anticancer agent 5-FU.[32,33] It is also known that quiescent leukemic CSCs are $CD71^-$, and CD71 expression is closely related to cell cycle status as CD71 is expressed mainly in proliferative cells.[27,34] In the present study, $CD71^-$ cells were enriched after 5-FU treatment and accumulated during the G0/G1 cell cycle phase. These findings are compatible with previous studies of leukemic CSCs and suggest that the $CD71^-$ cell fraction survives after treatment with anticancer agents and contributes to cancer regrowth and recurrence.

In limiting dilution and serial transplantation assays, the $CD71^-$ cell fraction showed a comparatively higher ability to form tumors than the $CD71^+$ cell fraction. Although data from the limiting dilution and serial transplantation experiments were not as clear as we expected, at least in the $CD71^-$ fraction, there was a characteristic cell population that showed self-renewal and bipotentiality. In liver cancer, both semiquiescent CSCs and proliferating progenitor-like cells show tumorigenicity.[35] As with liver cancer, there may be a cancer hierarchy in gastric adenosquamous carcinoma. Given that the $CD71^-$ fraction has relatively high tumorigenic activity and only the $CD71^-$ fraction displays bipotentiality, there may be at least two cellular fractions in $CD71^-$ cells: semiquiescent bipotential CSCs and proliferating progenitor cells. Furthermore, when the mature cancer cell, without tumorigenicity, is in the G1 cell cycle phase, these cells may also be $CD71^-$. Thus, CD71 could be used to isolate a bipotential CSC-enriched population but is not sufficient to isolate a definitive CSC population by itself. Additional markers are required to identify and isolate definitive CSCs.

In the present study, $CD71^-$ cells showed high migratory and invasive ability. These data were also supported by a 3D culture of $CD71^-$ cells, which revealed that $CD71^-$ cells had globular features. Immunohistochemical analysis of clinical gastric adenosquamous carcinoma revealed that the invasive front of the cancer foci was negative for CD71. It is known that gastric adenosquamous carcinoma is highly metastatic in early stages and has poor prognosis.[36] $CD71^-$ cells have high potential for metastasis and produce cells of the squamous carcinoma phenotype, and metastatic lesions of adenosquamous carcinoma are mainly replaced by squamous carcinoma.[36] These observations suggest that $CD71^-$ cells are migratory and invasive, leading to metastasis in the early stages of cancer and later differentiating to squamous cell carcinoma and adenocarcinoma. Unfortunately, no metastatic lesions were observed in the $CD71^-$ or $CD71^+$ fraction when these were subcutaneously inoculated into mice. To assess the metastatic ability of these fractions physiologically and biologically in order to determine their clinical features, it may be better to inoculate cells into the subserosa of the stomach.

The present study, which was based on a cancer cell line, suggests that $CD71^-$ cells have important roles in cancer development; it has furthered our understanding of the cancer cell hierarchy. It is now necessary to confirm the roles of $CD71^-$ cells in the most common gastric cancer, adenocarcinoma.

ACKNOWLEDGMENT We thank T. Shimooka for excellent technical assistance. This work was supported in part by a grant from Core Research for Evolutional Science and Technology, and grants-in-aid for scientific research on priority areas (20012039) and for scientific research (S) (21229015) from the Ministry of Education, Culture, Sports, Science, and Technology, Japan.

DISCLOSURE There is no conflict of interest.

REFERENCES

1. Reya T, Morrison SJ, Clarke MF, Weissman IL. Stem cells, cancer, and cancer stem cells. *Nature.* 2001;414(6859):105–11.
2. Pardal R, Clarke MF, Morrison SJ. Applying the principles of stem-cell biology to cancer. *Nat Rev Cancer.* 2003;3(12):895–902.
3. Beachy PA, Karhadkar SS, Berman DM. Tissue repair and stem cell renewal in carcinogenesis. *Nature.* 2004;432(7015):324–31.
4. Polyak K, Hahn WC. Roots and stems: stem cells in cancer. *Nat Med.* 2006;12(3):296–300.
5. Tanaka K, Kiyohara Y, Kubo M, et al. Secular trends in the incidence, mortality, and survival rate of gastric cancer in a general Japanese population: the Hisayama study. *Cancer Causes Control.* 2005;16(5):573–8.
6. Takaishi S, Okumura T, Tu S, et al. Identification of gastric cancer stem cells using the cell surface marker CD44. *Stem Cells.* 2009;27(5):1006–20.
7. Nishii T, Yashiro M, Shinto O, Sawada T, Ohira M, Hirakawa K. Cancer stem cell-like SP cells have a high adhesion ability to the peritoneum in gastric carcinoma. *Cancer Sci.* 2009;100(8):1397–402.
8. Boku N. Chemotherapy for metastatic gastric cancer in Japan. *Int J Clin Oncol.* 2008;13(6):483–7.
9. Boku N. Gastrointestinal Oncology Study Group of Japan Clinical Oncology Group. Chemotherapy for metastatic disease: review from JCOG trials. *Int J Clin Oncol.* 2008;13(3):196–200.
10. Al-Hajj M, Wicha MS, Benito-Hernandez A, Morrison SJ, Clarke MF. Prospective identification of tumorigenic breast cancer cells. *Proc Natl Acad Sci USA.* 2003;100(7):3983–8.
11. Singh SK, Hawkins C, Clarke ID, et al. Identification of human brain tumour initiating cells. *Nature.* 2004;432(7015):396–401.
12. O'Brien CA, Pollett A, Gallinger S, Dick JE. A human colon cancer cell capable of initiating tumour growth in immunodeficient mice. *Nature.* 2007;445(7123):106–10.

13. Ricci-Vitiani L, Lombardi DG, Pilozzi E, et al. Identification and expansion of human colon-cancer-initiating cells. *Nature.* 2007;445(7123):111–5.
14. Joshi PA, Jackson HW, Beristain AG, et al. Progesterone induces adult mammary stem cell expansion. *Nature.* 2010;465(7299): 803–7.
15. Lathia JD, Gallagher J, Heddleston JM, et al. Integrin alpha 6 regulates glioblastoma stem cells. *Cell Stem Cell.* 2010;6(5):421–32.
16. Arai F, Hirao A, Ohmura M, et al. Tie2/angiopoietin-1 signaling regulates hematopoietic stem cell quiescence in the bone marrow niche. *Cell.* 2004;118(2):149–61.
17. Guan Y, Gerhard B, Hogge DE. Detection, isolation, and stimulation of quiescent primitive leukemic progenitor cells from patients with acute myeloid leukemia (AML). *Blood.* 2003; 101(8):3142–9.
18. Holyoake T, Jiang X, Eaves C, Eaves A. Isolation of a highly quiescent subpopulation of primitive leukemic cells in chronic myeloid leukemia. *Blood.* 1999;94(6):2056–64.
19. Lapidot T, Sirard C, Vormoor J, et al. A cell initiating human acute myeloid leukaemia after transplantation into SCID mice. *Nature.* 1994;367(6464):645–8.
20. Hogge DE, Lansdorp PM, Reid D, Gerhard B, Eaves CJ. Enhanced detection, maintenance, and differentiation of primitive human hematopoietic cells in cultures containing murine fibroblasts engineered to produce human steel factor, interleukin-3, and granulocyte colony-stimulating factor. *Blood.* 1996;88(10): 3765–73.
21. Yang G, Hisha H, Cui Y, et al. A new assay method for late CFU-S formation and long-term reconstituting activity using a small number of pluripotent hemopoietic stem cells. *Stem Cells.* 2002;20(3):241–8.
22. Tani H, Morris RJ, Kaur P. Enrichment for murine keratinocyte stem cells based on cell surface phenotype. *Proc Natl Acad Sci USA.* 2000;97(20):10960–5.
23. Calenic B, Ishkitiev N, Yaegaki K, et al. Magnetic separation and characterization of keratinocyte stem cells from human gingiva. *J Periodontal Res.* 2010;45(6):703–8.
24. Ohyama M, Terunuma A, Tock CL, et al. Characterization and isolation of stem cell-enriched human hair follicle bulge cells. *J Clin Invest.* 2006;116(1):249–60.
25. Yamazaki J, Mizukami T, Takizawa K, et al. Identification of cancer stem cells in a Tax-transgenic (Tax-Tg) mouse model of adult T-cell leukemia/lymphoma. *Blood.* 2009;114(13):2709–20.
26. Yalcintepe L, Frankel AE, Hogge DE. Expression of interleukin-3 receptor subunits on defined subpopulations of acute myeloid leukemia blasts predicts the cytotoxicity of diphtheria toxin interleukin-3 fusion protein against malignant progenitors that engraft in immunodeficient mice. *Blood.* 2006;108(10):3530–7.
27. Holyoake TL, Jiang X, Jorgensen HG, et al. Primitive quiescent leukemic cells from patients with chronic myeloid leukemia spontaneously initiate factor-independent growth in vitro in association with up-regulation of expression of interleukin-3. *Blood.* 2001;97(3):720–8.
28. Blair A, Hogge DE, Sutherland HJ. Most acute myeloid leukemia progenitor cells with long-term proliferative ability in vitro and in vivo have the phenotype CD34(+)/CD71(−)/HLA-DR−. *Blood.* 1998;92(11):4325–35.
29. Kalabis J, Oyama K, Okawa T, et al. A subpopulation of mouse esophageal basal cells has properties of stem cells with the capacity for self-renewal and lineage specification. *Clin Invest.* 2008;118(12):3860–9.
30. Croagh D, Phillips WA, Redvers R, Thomas RJ, Kaur P. Identification of candidate murine esophageal stem cells using a combination of cell kinetic studies and cell surface markers. *Stem Cells.* 2007;25(2):313–8.
31. Meng S, Tripathy D, Frenkel EP, et al. Circulating tumor cells in patients with breast cancer dormancy. *Clin Cancer Res.* 2004;10(24):8152–62.
32. Terpstra W, Ploemacher RE, Prins A, et al. Fluorouracil selectively spares acute myeloid leukemia cells with long-term growth abilities in immunodeficient mice and in culture. *Blood.* 1996;88(6):1944–50.
33. Chung SW, Chen H, Wong PM. Activation of quiescent ABL-transduced hemopoietic stem cells. *Oncogene.* 1996;13(11): 2397–405.
34. Sutherland R, Delia D, Schneider C, Newman R, Kemshead J, Greaves M. Ubiquitous cell-surface glycoprotein on tumor cells is proliferation-associated receptor for transferrin. *Proc Natl Acad Sci USA.* 1981;78(7):4515–9.
35. Haraguchi N, Ishii H, Mimori K, et al. CD13 is a therapeutic target in human liver cancer stem cells. *J Clin Invest.* 2010; 120(9):3326–39.
36. Yoshida K, Manabe T, Tsunoda T, Kimoto M, Tadaoka Y, Shimizu M. Early gastric cancer of adenosquamous carcinoma type: report of a case and review of literature. *Jpn J Clin Oncol.* 1996;26(4):252–7.

SSEA-3 as a novel amplifying cancer cell surface marker in colorectal cancers

YOZO SUZUKI[1], NAOTSUGU HARAGUCHI[1], HIDEKAZU TAKAHASHI[1], MAMORU UEMURA[1], JUNICHI NISHIMURA[1], TAISHI HATA[1], ICHIRO TAKEMASA[1], TSUNEKAZU MIZUSHIMA[1], HIDESHI ISHII[2], YUICHIRO DOKI[1], MASAKI MORI[1] and HIROFUMI YAMAMOTO[1]

Departments of [1]Gastroenterological Surgery and [2]Frontier Science for Cancer and Chemotherapy, Graduate School of Medicine, Osaka University, Suita, Osaka 565-0871, Japan

Received August 7, 2012; Accepted November 8, 2012

DOI: 10.3892/ijo.2012.1713

Abstract. Findings from studies on stem cells have been applied to cancer stem cell (CSC) research, but little is known about the relationship between ES cell-related cell surface markers and CSCs. In this study, we focused on stage-specific embryonic antigen 3 (SSEA-3), a marker of mesenchymal stem cells and Muse cells in colorectal cancer (CRC). Expression of SSEA-3 in human CRC cell lines and clinical specimens, specifically the relationship of SSEA-3 expression and the representative CSC markers (CD44, CD166, ALDH, CD24 and CD26) as well as with mesenchymal stem cell/Muse cell marker (CD105) were assessed. To characterize SSEA-3-expressing cells, tumorigenicity, sphere formation ability, expression of iPS genes (Oct4, NANOG, SOX2 and c-Myc), cell proliferation and cell cycle status were assessed. SSEA-3 expression was identified in Caco-2, DLD-1, HT-29, SW480 and HCT116, but not in CaR-1 cells. No significant relationship between SSEA-3 and other stem cell markers was detected. SSEA-3$^+$ cells showed increased tumorigenicity *in vivo*, but lower sphere formation ability *in vitro* than SSEA-3$^-$. iPS gene expression was not correlated with SSEA-3 expression status. SSEA-3$^+$ cells showed higher proliferative ability than SSEA-3$^-$ through enhanced cell cycles by decreased expression of $p21^{Cip1/Waf1}$ and $p27^{Kip1}$. Immunofluorescence analysis in clinical specimens indicated that expression of SSEA-3 is limited to stromal cells in normal mucosa but broad in poorly differentiated adenocarcinoma. These observations indicated that SSEA-3$^+$ cells in CRC have immature phenotype but decreased self-renewal ability and may function as tumor transient amplifying cells or delayed contributing tumor-initiating cells.

Correspondence to: Dr Naotsugu Haraguchi, Department of Gastroenterological Surgery, Graduate School of Medicine, Osaka University, 2-2 Yamadaoka, Suita, Osaka 565-0871, Japan
E-mail: nharaguchi@gesurg.med.osaka-u.ac.jp

Key words: stage-specific embryonic antigen 3, colorectal cancer, cancer stem cell, cell proliferation

Introduction

Recent vigorous research of somatic stem cells, embryonic stem (ES) cells and induced pluripotent stem (iPS) cells clarified several novel key regulators associated with cellular pluripotency, undifferentiated phenotype, self-renewal and stem cell maintenance. In cancer research, especially in cancer stem cell (CSC) research, some reports focused on the expression of pluripotency-associated factors and indicated their correlation with cancer cell aggressiveness (1), chemoradiotherapy resistance (2) and cancer stem-like cell properties (3), but little is known about the relationship between ES cell-related cell surface markers and cancer. In this study, we focused on stage-specific embryonic antigen 3 (SSEA-3) in colorectal cancer (CRC). SSEAs are globoseries glycolipids and are known to consist of 3 species; SSEA-1, 3 and 4. SSEA-1 and SSEA-4 were established through immunization of animals with human embryonic carcinoma cells, and SSEA-3 with 4- to 8-cell stage mouse embryos (4-6). SSEA-4 is similar to SSEA-3 in terms of structure; they share the same globoseries glycolipid but SSEA-4 has an additional terminal sialic acid moiety (7). SSEA-1 and SSEA-3/-4 are reportedly expressed on the surface of the murine (8-10) and human (11,12) pluripotent stem cells; inner cell mass of early embryos, ES cells and iPS cells, respectively. Though expression of SSEAs are thought to be attenuated during the process of differentiation, a recent report revealed that a small group of SSEA-3 expressing cells; multilineage differentiating stress enduring (Muse) cells, exist in adult skin fibroblasts and bone marrow stroma and that they possess stress tolerance and endogenous pluripotency (13). In cancer, expression of SSEA-1 is related to the poor prognosis (14) and tumor-initiating capacity in human glioblastoma (15), whereas the reduced expression of SSEA-4 is correlated with advanced tumor stages and poor tumor cell differentiation in ovarian cancer (16). In contrast to SSEA-1 and SSEA-4, there are only a few reports that have assessed SSEA-3 expression in cancer; in breast cancer, 77.5% of clinical breast cancer samples express SSEA-3 with a broad positive ratio (17), and in non-small cell lung cancer, SSEA-3 expression increases after exposure to multiple anti-cancer drugs (2). To the best of our knowledge, there are no reports that have clearly assessed SSEA-3 expression and its biological characteristics in gastro-

enterological cancer. Furthermore, there are no reports that have assessed SSEA-3 expression in association with CSC. In addition, human colorectal epithelial cells were shown to be SSEA-3 positive (17), implying that CRC tissue also contains SSEA-3 expressing immature subsets.

In this study, we assessed the existence of SSEA-3$^+$ cells in the cell lines of CRC. Next, we investigated the relationship between SSEA-3 expression and representative colorectal CSC or Muse cell marker, tumorigenic activity and sphere formation activity to assess for CSC-like properties. Then, we assessed the cell proliferation activity of SSEA-3$^+$ cells to characterize them. Finally, we assessed the distribution of SSEA-3$^+$ cells to confirm the existence of SSEA-3$^+$ cells in clinical specimens.

Materials and methods

Patients and tissue samples. Surgically resected CRC samples were obtained from 10 patients after informed consent from Osaka University Medical Hospital with approval of the research ethics board. All specimens were embedded in Tissue-Tek O.C.T. compound (Sakura Finetek, Tokyo, Japan), rapidly frozen by immersion in liquid nitrogen and stored at -80˚C.

Cell lines and culture. Human CRC cell line Caco-2, DLD-1, HCT116, HT-29 and SW480 were obtained from American Type Culture Collection (Manassas, VA) and Car-1 from Japanese Collection of Research Bioresources (Osaka, Japan). Caco-2 and Car-1 were maintained in Eagle's minimum essential medium (Wako Pure Chemical Industries, Tokyo, Japan), DLD-1, SW480 and NTERA-2 were maintained in Dulbecco's minimum essential medium (Wako Pure Chemical Industries), and HCT116 and HT-29 were maintained in McCoy's 5a medium (Invitrogen, Carlsbad, CA, USA), respectively supplemented with 10% fetal bovine serum (HyClone, Logan, UT, USA), penicillin and streptomycin (Pen-Strep; Invitrogen) at 37˚C in a humidified atmosphere containing 5% CO_2.

Immunofluorescent staining. The 7 μm thick frozen sections were obtained by using cryostat and fixed by 4% paraformaldehyde (Wako Pure Chemical Industries). After blocking, sections were incubated with rat anti-SSEA-3 monoclonal antibody (MAB4303, Millipore, Billerica, MA, USA) and Alexa Fluor 488 mouse anti-human E-cadherin (BD Pharmingen, San Diego, CA, USA). Alexa Fluor 594 goat anti-rat antibody (Invitrogen) was used as a secondary antibody. Rat IgM isotype (BD Pharmingen) was used as the control. Sections were mounted with ProLong Gold Antifade Reagent with DAPI (Invitrogen) and viewed with a fluorescent microscope (BZ-9000, Keyence, Osaka, Japan).

For immunocytochemistry, cells were cultured on 8-well culture slides (BD Falcon, Franklin Lakes, NJ) at the concentration of 20,000 cells/well for 24 h, fixed with 4% paraformaldehyde, then permealized with Triton X-100 (Sigma-Aldrich, St. Louis, MO, USA) and processed using the same protocol as the frozen sections.

Flow cytometry. Cells were dissociated with Accutase (Invitrogen), blocked with FcR blocking reagent (BD Biosciences) and incubated with antibodies as follows; anti-SSEA-3 (MAB4303, Millipore), anti-CD105 (APC-conjugated, BioLegend, San Diego, CA, USA), anti-rat IgM (APC-conjugated; Jackson ImmunoResearch Laboratories, West Grove, PA, FITC-conjugated; BD Biosciences, San Jose, CA, USA), anti-CD44, anti-CD24, anti-CD26 (conjugated form, BD Biosciences) and AldeFluor (Stemcell Technologies, BC, Canada). 7-AAD (BD Biosciences) was used to eliminate dead cells. Cells were analyzed and isolated by using FACSAriaII equipped with FACS Diva software (BD Biosciences).

RNA preparation and quantitative real-time PCR. Total RNA was isolated using TRIzol reagent (Invitrogen). In all cases, 1 μg of total RNA was reverse-transcribed with High Capacity RNA-to-cDNA Master Mix (Applied Biosystems, Foster, CA, USA) following the manufacturer's instructions. For quantitative assessments, real-time RT-PCR analysis was performed with the LightCycler TaqMan Master kit (Roche Diagnostics, Tokyo) and the LightCycler 480 system (Roche Applied Science, Indianapolis, IN, USA). The sequences of the primers used were as follows: *GAPDH* (NM_002046.3) sense primer 5'-AGCCACATCGCTCAGACAC-3' and antisense primer 5'-GCCCAATACGACCAAATCC-3'; *OCT3/4* (NM_203289.3) sense primer 5'-AATCCAGTCCCAGGACATCA-3' and antisense primer 5'-TGGCTGAATACCTTCCCAAA-3'; *NANOG* (NM_024865.2) sense primer 5'-ATGCCTCACACGGAGAC TGT-3' and antisense primer 5'-AGGGCTGTCCTGAATAA GCA-3'; *SOX2* (NM_003106.2) sense primer 5'-CTCCGGGA CATGATCAGC-3' and antisense primer 5'-CTGGGACAT GTGAAGTCTGC-3'; *c-MYC* (NM_002467.4) sense primer 5'-CACCAGCAGCGACTCTGA-3' and antisense primer 5'-GATCCAGACTCTGACCTTTTGC-3'.

Western blot analysis. Western blot analysis was performed as described previously (18). The following antibodies, at appropriate concentrations, were applied on membranes after the transfer of a sodium dodecyl sulfate-polyacrylamide gel (Bio-Rad Laboratories, Hercules, CA, USA): mouse anti-Oct4 monoclonal antibody (MAB4305, Millipore), anti-Nanog goat polyclonal antibody (R&D Systems, Minneapolis, MN, USA), anti-Sox2 rabbit polyclonal antibody (MBL, Nagoya, Japan), anti-cMyc, anti-$p21^{Cip1/Waf1}$, anti-$p27^{Kip1}$ and anti-cyclin D1 mouse monoclonal antibodies, anti-cyclin A2 and anti-cyclin B1 rabbit monoclonal antibodies (Santa Cruz Biotechnology, Santa Cruz, CA, USA), anti-p16 mouse monoclonal antibody (BD Pharmingen), and anti-cyclin E mouse monoclonal antibody (Calbiochem, La Jolla, CA, USA). Equal loading of the protein samples was confirmed by parallel western blots for actin with anti-actin rabbit polyclonal antibody (Sigma-Aldrich).

Cell cycle analysis. To synchronize cell cycle, double-thymidine block (DTB) method (19,20) was used. On 10 cm dishes, $1x10^6$ cells of HCT116 were cultured in media containing 2.5 mM thymidine (Sigma-Aldrich) for 18 h, placed in thymidine-free media for 12 h, and followed by an additional 18 h in thymidine containing media. Between the exchange of media, dishes were washed twice with PBS (Wako Pure Chemical Industries). Cell cycle was analyzed at 0, 4, 8, 16 and 24 h after release of block with PI/RNase Staining Buffer (BD Biosciences) on FACSAriaII and data analysis was performed using FlowJo software (Tree Star, Ashland, OR, USA).

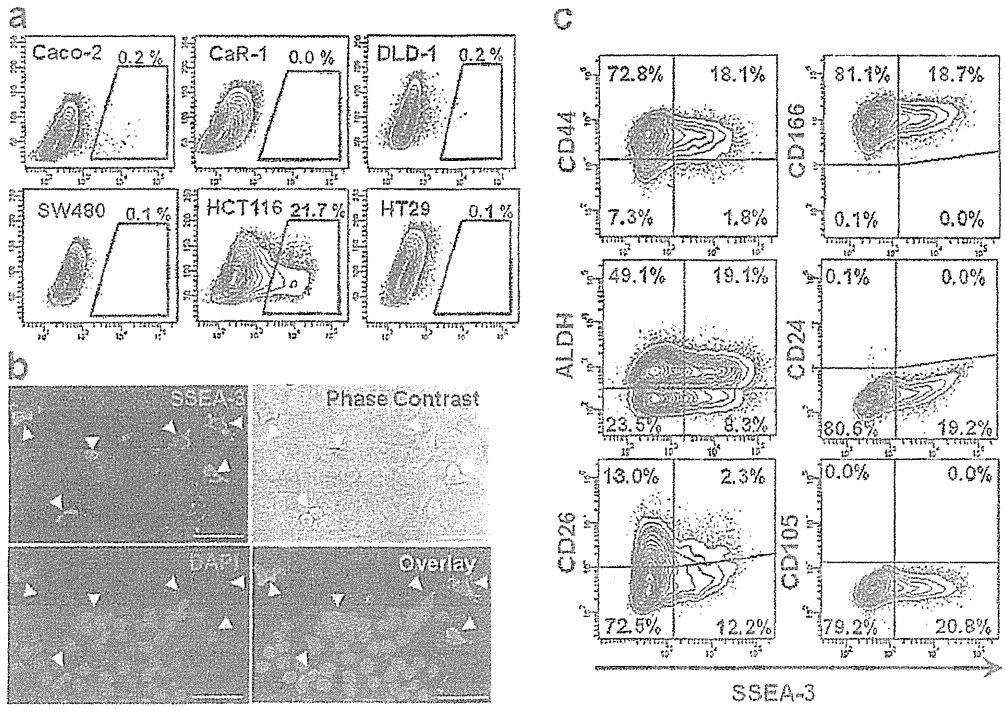

Figure 1. Flow cytometry analysis of human CRC cell lines with an anti-SSEA-3 antibody and other stem cell markers, and immunofluorescent staining of a human CRC cell line. (a) Representative dot plots of human CRC cell lines incubated with an anti-SSEA-3 antibody. Boxes show SSEA-3$^+$ cells, and the numbers above the boxes indicate the ratio of the SSEA-3$^+$ population in each cell line. (b) Immunofluorescent staining of HCT116 cells with anti-SSEA-3 (red) and DAPI (blue), and phase-contrast image. Arrow heads indicate SSEA-3$^+$ cells. Original magnification, x200. Scale bar, 50 μm. (c) Representative dot plots of HCT116 cells incubated with anti-SSEA-3 and anti-CD44, anti-CD166, anti-ALDH, anti-CD24, anti-CD26 and anti-CD105 antibodies. The numbers indicate the ratio of the population.

Sphere formation assay. Single cells of isolated SSEA-3$^+$ and SSEA-3$^-$ in HCT116 were seeded in 96-well ultra-low attachment plates (Corning, New York, NY, USA), cultured in mTeSR1 (Stem Cell Technologies) media without serum. Sphere formation was assessed 28 days after seeding. In each of the 48 wells, the number of formed spheres was calculated. This study was performed as triplicated study.

Cell proliferation assay. Isolated HCT116 SSEA-3$^-$ and SSEA-3$^+$ cells were put into 96-well plates at a density of $2x10^3$ cells in 100 μl medium per well, cultured for 24 h in McCoy's 5A medium supplemented with 10% FBS, and then cultured for an additional 24, 48, 72 and 96 h. Cell proliferation was assessed with Cell Counting kit-8 incorporating WST-8 (Dojindo Molecular Technologies, Kumamoto, Japan) following the manufacturer's instructions with a plate reader (Model 680XR; Bio-Rad Laboratories).

Xenotransplantation. To assess tumorigenic properties, each of the 5,000 and 1,000 SSEA-3$^-$ and SSEA-3$^+$ cells were inoculated into dorsal flanks of 8-week-old NOD/SCID mice (CREA, Tokyo) with a mixture of Matrigel matrix (BD Biosciences). Tumor growth was monitored every three or four days by measurement with calipers and the volume of the subcutaneous tumor was calculated by the following formula; $v = l \times w^2/2$, where v = volume, l = length and w = width (21).

Statistical analysis. The relationships among gene expressions, cell counts, and tumor volume were analyzed using Student's t-tests. All tests were analyzed with JMP 9 software (SAS Institute, Cary, NC, USA). A value of $P<0.05$ was taken as statistically significant.

Results

SSEA-3 expression in CRC cell lines. To assess SSEA-3 expression in CRC, flow-cytometric analysis was performed on 6 CRC cell lines. It indicated that a small number of SSEA-3$^+$ population existed in most of the CRC cell lines; 0.1 to 0.2% in Caco-2, DLD-1, HT-29 and SW480. Among those tested, HCT116 had the highest expression level; it had as much as 21.7±8.3% SSEA-3$^+$ population. In CaR-1 cells, expression of SSEA-3 could not be identified in this triplicate study (Fig. 1a). To confirm SSEA-3 expression in HCT116 cells, immunofluorescent staining of SSEA-3 was performed. Consistent with the results of flow cytometric analysis, a small number of HCT116 cells expressed SSEA-3 (Fig. 1b). In this study, HCT116 was used for the following analyses because it had abundant SSEA-3$^+$ cells and it was easy to isolate SSEA-3$^-$ and SSEA-3$^+$ populations.

Correlation of SSEA-3 and stem cell markers. To clarify the correlation between SSEA-3 and representative colorectal